Mechanisms of Gadographene-Mediated Proton Spin Relaxation
Supporting Information

Andy H. Hung,[§,†] Matthew C. Duch,[§,‡] Giacomo Parigi,[‖] Matthew W. Rotz,[†] Lisa M. Manus,[†] Daniel J. Mastarone,[†] Kevin T. Dam,[†] Colton C. Gits,[‡] Keith W. MacRenaris,[†] Claudio Luchinat,[‖] Mark C. Hersam,[*,‡] and Thomas J. Meade[*,†]

[†]Department of Chemistry, Molecular Biosciences, Neurobiology, Biomedical Engineering, and Radiology, Northwestern University, 2145 Sheridan Road, Evanston, Illinois 60208-3113, United States

[‡]Department of Materials Science and Engineering and Department of Chemistry, Northwestern University, 2220 Campus Drive, Evanston, Illinois 60208-3108, United States

[‖]CERM and Department of Chemistry, University of Florence, via L. Sacconi 6, 50019 Sesto Florence, Italy

Table of Contents

1. Materials and Methods

1.1 Preparation of Gd(III) Graphene, Gd(III) GO, and analogues utilizing other metals

1.1.1 Gd(III) Graphene Preparation

Batches of sodium cholate (SC)-dispersed graphite were prepared by adding 7 grams of graphite (3061 grade, Asbury Graphite Mills) to 70 mL of 2% w/v aqueous sodium cholate (from ox or sheep bile, ≥99%, Sigma-Aldrich) solution in a ~120 mL stainless steel beaker. This mixture was ultrasonicated with a Fisher Scientific Model 500 Sonic Dismembrator using a 1/2" diameter tip, while being chilled in an ice bath. By varying the sonication length and power, four different grades of samples were produced: low (45 min at 40 W), medium (1 h at 55 W), high (1 h at 70 W), and very high (16 h at 55 W) sonication dose. The resulting solution was centrifuged in a Beckman Coulter JS-7.5 rotor with a Beckman Coulter J26-XPI at 5000 rpm (~4,620g) for 30 min to remove any large particles or aggregates. The top 90% of the supernatant was retained and its graphene concentration determined using an average absorption coefficient of 2460 mL mg^{-1} m^{-1} at 660 nm.[1]

To produce an individual sample, a volume of solution containing 8 mg of dispersed graphene was mixed with acetone at a ratio of 1:4 graphene solution to acetone, in order to aggregate the graphene and remove the SC surfactant from the graphene surface. The solution was centrifuged, as described previously, for 30 min at 5000 rpm, during which the aggregated graphene was removed from the solution. After the supernatant was decanted, a total of 200 mL of DI was added to the pelleted graphene, and the mixture was vortexed for 60 sec. The mixture was then centrifuged for 30 min at 5000 rpm to remove the graphene from solution. This process of DI addition, vortexing, centrifugation, and supernatant removal was repeated 4 times to ensure any remaining acetone and surfactant was removed, and the remaining pellet was retained for further processing.

A method for Gd(III) functionalization of single-walled carbon nanotubes has previously been reported,[2] and was used as the basis for Gd(III) functionalization of graphene. 8 mL of 1 mg/mL aqueous $GdCl_3$ was added (to produce samples with other metal analogues, the appropriate 1 mg/mL aqueous solution was substituted) to the graphene pellet from the previous step, and the mixture was vortexed for 60 sec. The sample was then bath sonicated for 1 h and left undisturbed for 12 h. The sample was centrifuged for 30 min at 5000 rpm to remove the Gd(III)-graphene from solution and the supernatant was decanted. 50 mL of DI was added to the pelleted graphene, and the mixture was vortexed for 60 sec. The mixture was centrifuged again for 30 min at 5000 rpm. This process of DI addition, vortexing, centrifugation, and supernatant removal was repeated 4 times to ensure any remaining free Gd^{3+} and aqueous Cl^- was removed, and the remaining pellet was retained for further processing. Reference samples were prepared using the same method, except DI was added to the pellet instead of aqueous $GdCl_3$.

In order to produce dispersed Gd(III)-graphene samples, the pellet from the previous step was added to 8 mL of either 2% w/v aqueous sodium cholate (from ox or sheep bile, ≥99%, Sigma-Aldrich) solution or 2% w/v aqueous Pluronic F108NF (BASF Corporation) solution. The sample was horn sonicated using a Fisher Scientific Model 500 Sonic Dismembrator with an 1/8" tapered horn tip for 1 hour at 20% amplitude (~10 W), while being chilled in an ice bath. Finally, the sample was centrifuged using an Eppendorf Model 5424 Microcentrifuge with a FA-45-24-11 fixed-angle rotor for 30 min at 15,000 rpm (~21,000 g) to remove any remaining large aggregates, and the top 90% of the supernatant was retained as the final sample.

1.1.2 Gd(III) Graphene Oxide Preparation

Graphene oxide was prepared using a modified Hummer's method[3] as previously described.[4] Briefly, 115 mL of concentrated sulfuric acid (Mallinckrodt Baker) were cooled in an ice water bath, and

5 g of natural graphite flakes (3061 grade material, Asbury Graphite Mills) were added to the chilled sulfuric acid. 15 g of $KMnO_4$ were added to the mixture, which was subsequently heated to 35°C. The mixture was kept at 35°C and stirred for two hours. Then, 230 mL of DI water were added, and 15 minutes later the reaction was terminated by the addition of 700 mL of DI water. Following termination of the reaction, 12.5 mL of 30% H_2O_2 solution were slowly added.

The mixture was then vacuum filtered, the GO was washed with 1.25 L of 1:10 HCl solution to remove metal ions, and further washed with 4 L of DI water. The resulting material was then suspended in 250 mL of DI water. Batches of 8 mL of the mixture from the previous step, diluted to ~4 mg/mL carbon, were sonicated in a 16 mL vial by a Fisher Scientific Model 500 Sonic Dismembrator with an 1/8" tapered horn tip for 1 hour at 20% amplitude (~10 W), while cooled using an ice water bath. The solution was then centrifuged in an Eppendorf Model 5424 Microcentrifuge with a FA-45-24-11 fixed-angle rotor for 10 minutes at 15,000 rpm (~21,000 g) to remove any remaining large aggregates. The top 90% of the solution was retained as dispersed graphene oxide, and its concentration was determined using an average absorption coefficient of 3650 mL mg^{-1} m^{-1} at 300 nm.[4]

To produce Gd(III) functionalized material, a volume containing 16 mg of dispersed graphene oxide from the previous step was centrifuged in a Beckman Coulter JS-7.5 rotor with a Beckman Coulter J26-XPI at 5000 rpm (~4,620g) for 12 h to aggregate the graphene oxide. The supernatant was decanted and the pellet was retained for further processing. The material was then Gd(III) functionalized as described in the previous section, where 16 mL of 1 mg/mL aqueous $GdCl_3$ (or other aqueous metal solution) was added and the solution was bath sonicated for 1 h, and allowed to sit undisturbed for 12 h.

The samples were then washed with 4 steps of DI addition, vortexing, centrifugation, and decanting as previously described, except the samples were centrifuged for 12 h at 5000 rpm (as compared to 30 min at 5000 rpm for graphene samples). This is due to the hydrophilicity of GO, which

resulted in solutions with greatly increased stability (as compared to hydrophobic graphene), and therefore required significantly longer centrifugation times to fully pellet. 8 mL of DI was added to the final pellet, which was then sonicated using a Fisher Scientific Model 500 Sonic Dismembrator with an 1/8" tapered horn tip for 1 hour at 20% amplitude (~10 W), while being chilled in an ice bath. Finally, the material was centrifuged for 10 min at 15,000 rpm (~21,000 g) to remove any remaining large aggregates, and the top 90% of the supernatant was retained as the final sample.

1.2 Preparation of Gd(III)-Complex Graphene and Gd(III)-Complex GO

1.2.1 Preparation of Partially Reduced Graphene Oxide

Similar to a previously published method,[5] 10 mL of 3M NaOH was added to 10 mL of ~4 mg/mL dispersed graphene oxide solution, and then bath-sonicated for 6 hours. The rest of the procedure follows that of other GO-based samples closely. The NaOH-treated GO was centrifuged in a Beckman Coulter J26-XPI centrifuge at 5000 rpm (~4,620 g) for 12 h to aggregate the GO. After the supernatant was decanted, the pellet was then washed with 4 steps of DI addition, vortexing, centrifugation at 5000 rpm for 12 h, and decanting, repeated 4 times. 8 mL of DI was added to the final pellet, which was then sonicated using a Fisher Scientific Model 500 Sonic Dismembrator with a 1/8" tapered horn tip for 1 hour at 20% amplitude (~10 W), while being chilled in an ice bath. Finally, the material was centrifuged for 10 min at 15,000 rpm (~21,000 g) to remove any remaining large aggregates, and the top 90% of the supernatant was retained as the final sample. Based on studies by Fernandez-Merino, et al.,[6] and Rourke et al.,[7] the treatment of GO by strong base strips the GO of oxidative debris to achieve a partially reduced, conductive material.

1.2.2 Synthesis of Gd(III)-DTPA-NH_2 (Gd(III) [(carboxymethyl)iminobis(ethylenenitrilo)]tetraacetic acid mono(2-aminobutylamide) monohydrate)

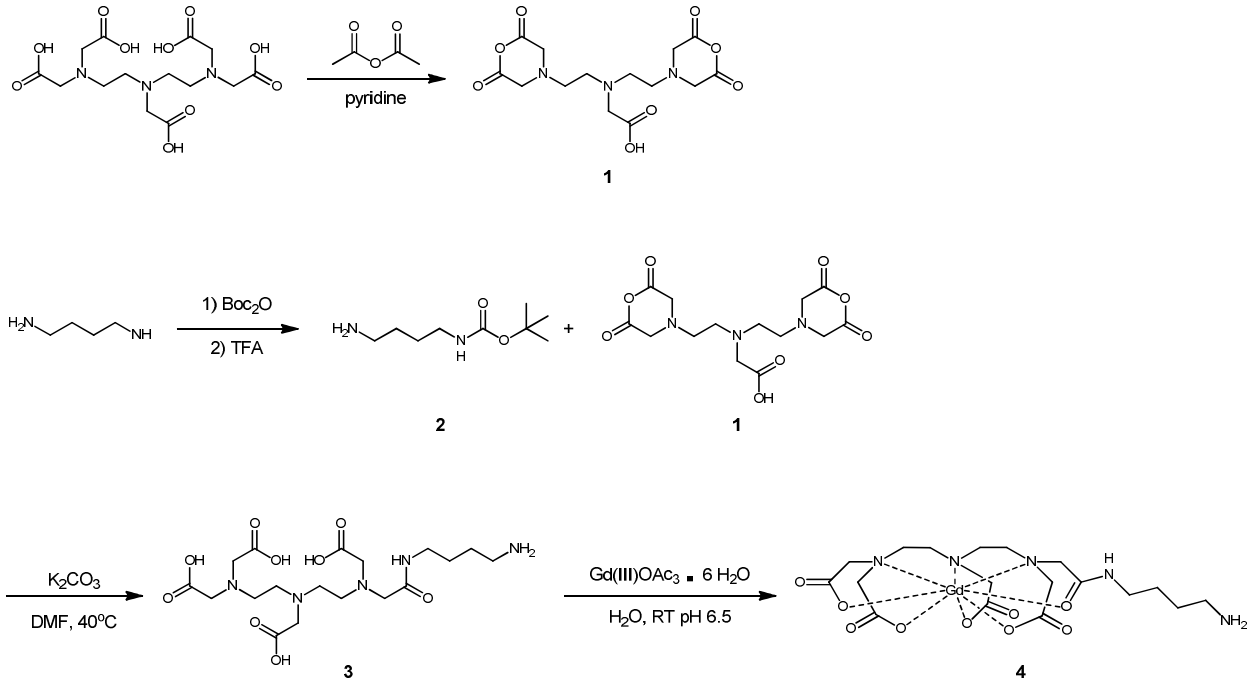

Scheme S1. Synthetic strategy for Gd(III)-DTPA-NH_2 modified from the work by Essien et al.[8]

*Diethylene triamine pentaacetic acid bisanhydride - (**1**)*

To a flame-dried 100 mL two neck round-bottom flask with a magnetic stir bar is added diethylene triamine pentaacetic acid (12.41g, 31.5 mmol) and pyridine (18 mL) under N_2 atmosphere with stirring. Freshly distilled acetic anhydride (14.51g, 142 mmol) is then added. The reaction is maintained under nitrogen, heated to 65°C, and stirred for 24 hrs. Over this time, the reaction turns to dark brown with a visible white suspension. White solid product is filtered from supernatant and washed with cold diethyl ether. After thorough washing, pure product is obtained as a white powder (7.89g, 70.1%).

^{1}H NMR (500 MHz, DMSO) δ 3.72 (s, 1H), 3.31 (s, 0H), 2.76 (t, *J* = 6.3 Hz, 1H), 2.60 (t, *J* = 6.2 Hz, 1H). ^{13}C NMR (126 MHz, DMSO) δ 171.95, 165.90, 54.60, 52.64, 51.73, 50.70.

*tert-Butyl 4-aminobutylcarbamate - (**2**)*

The synthesis of compound **2** is based on a modified literature procedure.[9] To a dry, 250 mL two-necked round-bottom flask containing a stir bar is added 1,4 diaminobutane (6.49g, 73.7 mmol) and dry 1,4 dioxanes under a nitrogen atmosphere with stirring. To this flask is added a 100 mL dropping funnel, containing di-*tert*-butyl dicarbonate (2.05g, 9.4 mmol) and 1,4 dioxanes (40 mL) under nitrogen, mixed by repeated aspiration by syringe. The di-*tert*-butyl dicarbonate is added over 3 hours with stirring at ambient temperature, and is stirred a further 12 hours under nitrogen. After this time, a clear solution containing white solid is evaporated to dryness, and then re-dissolved in water (50 mL). This mixture is then filtered to remove solid bis-substituted product and is extracted with dichloromethane (5 x 25 mL). The organic fraction is then dried using sodium sulfate, and is thoroughly evaporated to remove the starting 1,4 diaminobutane, and is further stored under vacuum overnight as a clear oil (1.72g, 97%).

^{1}H NMR (500 MHz, $CDCl_3$) δ 4.73 (s, 1H), 3.13 (d, *J* = 6.3 Hz, 2H), 2.71 (t, *J* = 6.8 Hz, 2H), 1.55 – 1.46 (m, 4H), 1.44 (s, 9H). ^{13}C NMR (126 MHz, $CDCl_3$) δ 79.02, 42.13, 41.85, 40.42, 30.93, 28.42, 27.48.

*[(carboxymethyl)iminobis(ethylenenitrilo)]tetraacetic acid mono(2-aminobutylamide) - (**3**)*

To a 500 mL two-necked round-bottom flask with a magnetic stir bar is added diethylene triamine pentaacetic acid bisanhydride (**1**, 4.56g, 12.8 mmol) and dimethylformamide (250 mL) under a nitrogen atmosphere. The mixture is stirred at 40°C for about one hour until bisanhyrdride **1** dissolves, at which time is added K_2CO_3 (0.44g, 12.8 mmol). Using a dropping funnel, *tert*-Butyl 4-aminobutylcarbamate (**2,** 0.60 g, 3.2 mmol) in dimethylformamide (100 mL) is added over 12 hours.

Upon complete addition of protected diamine **2**, the mixture is allowed to stir a further 12 hours at 25°C. The crude mixture is filtered to remove excess carbonate, and evaporated to dryness as an orange oil. To the crude product is added trifluoroacetic acid (50 mL) with stirring overnight at 25°C. Complete deprotection is observed after 12 hours. Trifluoroacetic acid is evaporated by blowing with nitrogen, followed by dissolution in methanol (3 x 25 mL) and further rotary evaporation for complete removal of acid. The crude product is dried to a dark brown oil, which is stored under vacuum overnight and taken forward with no further purification.

ESI-MS (*m/*z) observed: 462.2, calculated: 462.2$[M - H]^-$.

*Gd(III) [(carboxymethyl)iminobis(ethylenenitrilo)]tetraacetic acid mono(2-aminobutylamide) monohydrate – Gd(III)-DTPA-NH_2 – (**4**)*

To a 250 mL round-bottom flask containing a magnetic stir bar is added crude (**3**) and water (25 mL). Gd(III) Acetate · 6 H_20 (6.34g, 15.6 mmol) is then added, at which time the solution pH drops to pH 1.5. The mixture is brought to and maintained at pH 6.5 using 2.5M aqueous NaOH and stirred for 24 hours at 25°C. The crude mixture is purified by semipreparative HPLC on a reverse phase column (Varian Prostar 500 system with a Waters 19 × 250 mm Atlantis C18 Column), eluting via the use of the following water (A) / methanol (B) separation method: initial conditions of 0% B were held constant for 5 min, followed by a ramp to 7% B over 30 seconds, and then continuous isocratic flow from 5.5 – 25 minutes. At 25 min the method ramps to 100 % B for 5 min followed by return to 0% B in a further 5 minutes. The desired product elutes from 14 – 15.2 minutes as monitored by UV-Vis at 201/210 nm and is collected and freeze dried. Yield: 0.565 g (40 %).

ESI-MS (*m/*z) observed: 617.1, calculated: 617.1 $[M]^-$.

1.2.3 Synthesis of Gd(III)-DO3A-NH_2 (Gd(III) 2,2',2''-(10-(6-(amino)hexyl)-1,4,7,10-tetraazacyclododecane-1,4,7-triyl)triacetate)

Gd(III)-DO3A-NH_2 was synthesized using procedures previously developed by our group.[10] ESI-MS (m/z) observed: 601.1990, calculated: 601.1979 [M + H]+. Elemental Analysis calculated for Na[C20H36GdN5O6]·H2O·TFA: C, 35.01; H, 5.21; N, 9.28. Found: C, 35.16; H, 5.39; N, 9.16.

1.2.4 Gd(III)-Complex Graphene and Gd(III)-Complex GO

Method for the preparation of Gd(III)-DO3A Graphene 2%SC and 2%PL was devised to couple Gd(III)-DO3A-NH_2 to the edge carboxylate groups of graphene via carbodiimide chemistry. In a 2 mL microcentrifuge tube, 1-Ethyl-3-(3-dimethylaminopropyl)carbodiimide (EDC·HCl, 32 mg, 167 µmol, in 100 µL PB), Gd(III)-DO3A-NH_2 (10 mg, 17 µmol, in 100 µL PB), graphene (0.5 mg in 2%SC or 2%PL solution), and 10 mM pH 7.2 phosphate buffer (PB) were added to a final volume of 1.5 mL. The final concentration of PB depended on the volume of graphene solution added and was typically < 5 mM. For Gd(III)-DO3A Graphene 2%PL Preparation 1C (Table S1), water was used instead of PB. The mixture was left overnight at room temperature under gentle rocking, and then sonicated for 15-60 min. Excess reagents were removed by spin dialysis using an Amicon Ultra-4 100,000 MWCO centrifugal filter unit (Millipore, Billerica, MA). Samples were diluted to 4 mL with 2%SC or 2%PL in milli-Q water and centrifuged at 3000 rpm for 5-15 min in an Eppendorf Model 5810R centrifuge equipped with an A-4-62 swinging bucket rotor until the volume of the retentate was less than 500 µL. Graphene was often found trapped on the filter membranes and was re-suspended between centrifugations. Washing was repeated until the T_2 of the filtrate was within 10% of the diamagnetic reference and stable over three rounds of washing. 8-13 washes were required to meet these criteria. The washed gadographenes were sonicated (< 1 hour) and centrifuged at 3000 rpm for up to 20 min (Thermo Scientific, Model

Legend Micro 21R) to remove any large aggregates. The supernatant was recovered as the final agent and stored at room temperature.

Method for the preparation of Gd(III)-DO3A GO/rGO and Gd(III)-DTPA GO/rGO was devised to couple Gd(III)-DO3A/DTPA-NH_2 to the basal plane of GO via epoxide ring-opening.[11-14] The rGO used was only partially reduced.[6,7] In a 2 mL microcentrifuge tube, GO/rGO (0.5 mg in milli-Q water), triethylamine (TEA, 11 μL, 79 μmol), milli-Q water, and Gd(III)-DO3A/DTPA-NH2 (10 mg, 17 μmol, in 100 μL milli-Q water) were added, in that order, to a final volume of 1.25 mL. The mixture was confirmed to be basic by a pH strip and left rocking overnight. Excess reagents were removed by centrifuging at 14,800 rpm (21,100 g) for at least 20 min to form a pellet, and then spin-dialyzing the colored supernatant using an Amicon filter at 3000 rpm for 10 min (Eppendorf Model 5810R centrifuge equipped with an A-4-62 swinging bucket rotor), repeated at least once; the retentate was returned along with NaOH-basified milli-Q water (pH 10) to the original microcentifuge tube to re-suspend the pellet. This washing process was repeated until the T_2 of the spin-dialysis filtrate was within 20% of the diamagnetic reference and stable over three rounds of washing. 7-10 washes were required to meet these criteria. The washed gadographenes were centrifuged at 3000 rpm for 20 min (Thermo Scientific Model Legend Micro 21R) to remove any large aggregates. The supernatant was recovered as the final agent and stored at room temperature.

1.3 60 MHz relaxivity measurement

All relaxivities were measured on a 60 MHz (1.41 T) Bruker mq60 minispec relaxometer (Bruker Canada, Milton, Ontario, Canada) at 310 K. For T_1 measurements, an inversion recovery pulse sequence was used. For T_2 measurements, a Carr-Purcell-Meiboom-Gill pulse sequence with 1 ms 90^o-180^o pulse separation was used. Two-fold serial dilutions by milli-Q water, 2%SC, or 2%PL were performed on each sample to yield four different concentrations, in addition to the solvent diamagnetic reference for a total

of five data points per sample. Relaxation rate R_i ($1/T_i$), i=1,2, was plotted against Gd(III) concentration and linear-fitted to yield a slope reported as relaxivity. Gd(III) concentration was measured by ICP-MS. SC and PL did not significantly affect relaxation times at the concentrations used (Table S6).

Relaxivities were corrected for iron or carbon by subtracting their contribution to each measured relaxation rate according to eq [S1] and re-performing the linear fit.

$$R_{i,corrected} = R_{i,measured} - r_{i,Fe\ or\ C}[Fe\ or\ C],\ i=1,2 \quad [S1]$$

$r_{i,Fe\ or\ C}$ is the relaxivity of Fe or carbon nanomaterial measured in graphene or GO samples free of Gd(III) (Table S1). For a discussion on this correction method, see Supplementary Note S1.

1.4 Gd(III) loading measurement

Graphene and GO concentrations were measured by optical absorbance using extinction coefficients 2460 mL m^{-1} mg^{-1} at 660 nm[1] and 3650 mL m^{-1} mg^{-1} at 300 nm,[4] respectively. The measured nanomaterial concentration was converted to carbon concentration by atomic mass. For GO, the carbon concentration was overestimated because oxygen was not taken into account in the conversion. As a result, Gd(III) loading (written as per 10,000 C) in GO samples were under-estimated. Optical absorbance measurements were performed on a Varian Cary 5000 spectrophotometer with solvent background subtraction. The concentration of Gd(III) was measured by ICP-MS. Loading was obtained by taking the ratio of Gd(III) concentration to carbon concentration.

1.5 Dynamic Light Scattering (DLS) size measurement

Hydrodynamic size was obtained on a Malvern Instruments Zetasizer Nano Series Nano-ZS with Dispersion Technology Software v5.03 (Worcestershire, United Kingdom). Samples were measured in SARSTEDT clear polystyrene 10 × 10 × 45 mm cuvettes at room temperature. For data to be admissible, measurement of each sample must prove reproducible over two different agent concentrations (apart

by a two-fold dilution) and three different detector positions for a total of six measurement conditions; the polydispersity index must not exceed 0.4; raw data must meet quality criteria recommended by the software both as individual runs and as measurement groups. Z-average was reported as the hydrodynamic size, and the standard error for all samples stayed within 2%. The measured size is only intended to be used as a relative figure because the nanomaterials characterized are not spherical.

1.6 Atomic Force Microscopy (AFM) size measurement

Atomic force microscopy was performed as previously described.[4] Briefly, Si wafers with 100 nm thick oxide were functionalized with a monolayer of 2.5 mM (3-aminopropyl) triethoxysilane (APTES). Graphene or GO solutions were diluted to ~0.01 mg/mL with DI water, placed on the APTES functionalized substrates for 10 min, and were subsequently washed twice with DI water. To avoid issues with residual APTES, the GO samples were heat treated at 250 °C in air for 30 min. As this heat treatment was insufficient to remove SC and PL from the graphene samples, all graphene samples were heat treated in air at 275 °C for 60 min. AFM images were obtained via a Thermo Microscopes Autoprobe CP-Research AFM in tapping mode with conical probes (MikroMasch, NSC36/Cr-Au BS). Several random locations on each sample were imaged and showed little variation. All images were obtained using identical scanning conditions. Only flakes larger than 400 nm^2 were analyzed, as smaller features could not be definitively classified as flakes or residue. Also, any features taller than 5 nm were ignored as they appeared to be large aggregates. The measured sizes were fitted to a log-normal distribution, and the mean was reported.

1.7 Binding constant measurement

The Gd(III) binding constant of each ionic gadographene was measured by competition against three different ligands in addition to carbonate precipitation for a total of four estimates. The ligands are 1,2-daminoethane-N,N,N',N'-tetraacetic acid (EDTA), 1,3-daminopropane-N,N,N',N'-tetraacetic acid

(TMTA), and 1,6-daminohexane-N,N,N',N'-tetraacetic acid (HMDTA). Ligands or $NaHCO_3$ were titrated in excess into a sample of gadographene at 310 K. To ensure that the measurements were not influenced by pH, the prepared stock ligand solutions were neutralized by NaOH or HCl prior to titration. In addition, the gadographene samples were buffered by 100 mM HEPES at pH 7.4 and monitored for pH changes. pH shifted by less than 0.5 after titration in all cases except in the case of $NaHCO_3$, which reached a final pH of 9.0. A control study had shown Gd(III) ions to remain bound to the carbon nanomaterial at this pH (unpublished data). Each titration step was allowed to equilibrate for at least 45 min before both the longitudinal (T_1) and the transverse (T_2) relaxation times were measured following vortexing. Eq [S2] was used to calculate the fraction of Gd(III) displaced by the competitor,

$$R_{i,total} = r_{i,GdC}[Gd]_C + r_{i,GdL}[Gd]_L + r_{i,C}[C] + R_{i,dia},\ i=1,2 \qquad [S2]$$

$R_{i,total}$ is the measured relaxation rate ($1/T_i$), $R_{i,dia}$ is the relaxation rate of the solvent, $r_{i,GdC}$ is the relaxivity of the gadographene after correcting for the carbon backbone contribution, $r_{i,GdL}$ is the relaxivity of the Gd(III)-ligand or $Gd_2(CO_3)_3$ measured in separate control experiments, $r_{i,C}$ is the relaxivity of the carbon nanomaterial without Gd(III), $[Gd]_C$ and $[Gd]_L$ are the concentration of Gd(III) bound to carbon nanomaterial and competing ligand (or CO_3), respectively, and [C] is the concentration of graphene or GO. $[Gd]_C$ and $[Gd]_L$ add to $[Gd]_{total}$, which was measured by ICP-MS. The fraction of Gd(III) displaced by the competing ligands was calculated as $[Gd]_L/[Gd]_{tot}$. The increased volume from titration was taken into account in this calculation.

The fraction of Gd(III) displaced as a function of competitor concentration was analyzed mathematically to obtain the Gd(III) binding constant (K_b) to the corresponding carbon nanomaterial. In the presence of carbonate, the ability of graphene or GO to solubilize Gd(III) from the $Gd_2(CO_3)_3$ precipitate is a reflection of K_b. The solubilizing constant (K_{sol}) is related to K_b via eq [S3]-[S6][15]

$$K_{sol} \equiv \frac{[Gd]_C}{[Binding\ site]_C} \quad [S3]$$

$$log\ K_{sol} = log\ K_b + log\ [Gd]_{free} - log\ (\alpha_L^{-1}) \quad [S4]$$

$$K_{sp} = [Gd]_{free}^2 [CO_3^{2-}]^3 \quad [S5]$$

$$pH = pK_a + \log\left(\frac{[CO_3^{2-}]}{[HCO_3^-]}\right) \quad [S6]$$

$[\text{Binding site}]_C$ is the concentration of Gd(III)-binding sites on the carbon nanomaterial, $[Gd]_{free}$ is the concentration of unbound Gd(III) that are in equilibrium with the bound species, α_L^{-1} is a term representing competing protonation equilibrium on the carbon nanomaterial, and K_{sp} is the solubility constant of $Gd_2(CO_3)_3$ (log K_{sp} = -32.2 at 25°C).[15]

For calculation, $[CO_3^{2-}]$ was solved for using $[HCO_3^-]$ assuming total dissociation of $NaHCO_3$, the known pK_{a2} = 10.33, and the measured pH with eq [S6]. $[Gd]_{free}$ was then calculated using eq [S5]. K_{sol} was obtained by eq [S3] using experimental data on the fraction of Gd(III) displaced from the carbon nanomaterials; by assuming saturation of the Gd(III)-binding sites on gadographenes (supported by unpublished data showing equal Gd(III) loading in gadographenes prepared at different Gd/C mixing ratios), $[\text{Binding site}]_C = [Gd]_{total}$. Once K_{sol} and $[Gd]_{free}$ were known, K_b was readily calculated by rearranging eq [S4]; K_b was underestimated because $\log(\alpha_L^{-1})$ was assumed to be zero due to difficulties in its estimation.

When Gd(III)-chelating ligands were used as competitors, an expression derived by Wang[16] for a system of two ligands competing for a single binding partner was used for analysis (eq [S7]-[S12]). The analytically closed expression is exact and correct even when the total concentrations of all the components are of the same order of magnitude.

$$K_L = 1/K_{GdL};\ K_d = 1/K_b \quad [S7]$$

$$= K_L + K_d + [L]_0 + [Binding\ site]_C - [Gd]_{total} \quad [S8]$$

$$b = K_d([L]_0 - [Gd]_{total}) + K_L([Binding\ site]_C - [Gd]_{total}) + K_L K_d \quad [S9]$$

$$c = -K_L K_d [Gd]_{total} \quad [S10]$$

$$\theta = arccos \frac{-2a^3+9ab-27c}{2\sqrt{(a^2-3b)^3}} \quad [S11]$$

$$[Gd]_L = \frac{[L]_0\left\{2\sqrt{(a^2-3b)}\cos\frac{\theta}{3}-a\right\}}{3K_L+\left\{2\sqrt{(a^2-3b)}\cos\frac{\theta}{3}-a\right\}} \quad [S12]$$

K_{GdL} is the conditional binding constant of the competing ligand towards Gd(III) with K_L being the corresponding dissociation constant; similarly, K_b is the Gd(III) binding constant of the carbon nanomaterial with K_d being the corresponding dissociation constant; $[L]_0$ is the total concentration of ligand titrated. The K_{GdL} of each ligand at pH 7.4 was calculated using eq [S13][17] based on literature potentiometry data.[18]

$$K_{GdL} = \frac{K_{GdL}^{formal}}{1+K_1[H^+]+K_1K_2[H^+]^2+\cdots+K_1K_2K_n[H^+]^n} \quad [S13]$$

K_{GdL}^{formal} is the formal stability constant, K_1, K_2,…K_n are the stepwise protonation constants of the ligand.

To obtain K_d and in turn, K_b, a plot of $[Gd]_L$ vs. $[L]_0$ was fitted to eq [S12]. $[Gd]_L$ was obtained by multiplying the displacement fraction obtained in eq [S2] by $[Gd]_{total}$. Dilution of $[Gd]_L$, $[Gd]_{total}$ = [Binding site]$_C$, and $[L]_0$ that resulted from titration was not taken into account in fitting to minimize complexity of implementation; the omission does not influence the order of magnitude estimate for K_b. For Gd(III) Graphene 2%SC and 2%PL, [Fe] was on the same order of magnitude as [Gd] (Table S1), and the two were analyzed together as [Metal]. EDTA and, presumably the other ligands, have stronger or weaker affinity towards Fe compared to Gd(III) depending on the oxidation state;[19] K_b would be overestimated by one or two orders of magnitude without consideration of Fe. Data fitting was done using Maple V14 (Waterloo, ON, Canada), which uses modified newton method from a least squares optimizer library provided by the Numerical Algorithms Group. The precision of fitting was set to 100 digits.

1.8 ^{17}O NMR water coordination number (q) and magnetic susceptibility (χ) measurement

^{17}O NMR studies were performed on a Varian Inova 400 MHz NMR spectrometer equipped with VnmrJ software at both 296 K and 353 K following a method developed by Djanashvili and Peters.[20] Briefly, the ^{17}O chemical shift (δ_{obs}) of ^{17}O-enriched D_2O (<3% v/v) with dissolved Gd(III)-agents was measured against a reference without Gd(III) and used to infer the number of coordinated waters (q) or Gd(III) magnetic susceptibility (χ) by using eq [S14].

$$\delta_{obs} = \delta_{\chi} + q \cdot P_m \cdot \delta_m \qquad [S14]$$

δ_{χ} is the chemical shift caused by the bulk magnetic susceptibility (BMS) that results from paramagnetic ions, P_m is the molar ratio of Gd(III)/H_2O, and δ_m is the chemical shift of a Gd(III)-bound water molecule.

When NMR is performed with locking, the effect of BMS is corrected for, and $\delta_{\chi} = 0$. For Gd(III), δ_m can be approximated as $\langle S_z \rangle \cdot F = 31.5 \cdot -2.407 \cdot 10^4 \cdot T^{-1}$, where F is a term characteristic of ^{17}O, and T is the temperature in Kelvins. Accordingly, eq [S14] can be rewritten as the following to calculate q,

$$q = \frac{\delta_{obs}}{31.5\, P_m} \cdot \frac{T}{-2.407 \cdot 10^4} \qquad [S15]$$

For magnetic susceptibility, the ^{17}O chemical shift of each sample was measured with and without locking to obtain δ_{χ}. Using δ_{χ}, the effective magnetic moment (μ_{eff}) of Gd(III) can be calculated with eq [S16],

$$\delta_{\chi} = \frac{4\pi s[Gd]}{T}\left(\frac{\mu_{eff}}{2.84}\right)^2 \times 10^3 \qquad [S16]$$

s is a shape factor (s = 0, 1/3, -1/6 for a sphere, a cylinder parallel to, or a cylinder perpendicular to the main field, respectively) and [Gd] is in molars. Eq [S16] assumes that the susceptibility (χ) of Gd(III) behaves according to Pauli paramagnetism. Therefore, an agreement between the calculated and the

theoretical μ_{eff} indicates a value for χ that is consistent with the expectation for Gd(III) ions, whereas a disagreement suggests potentially novel modulations of the Gd(III) magnetic susceptibility.

Due to limitations in sample preparation, the experiments were performed under conditions outside of the recommendations by Djanashvili and Peters; namely, the measurements were performed directly on Gd(III) despite line broadening effects and at very low concentrations (approximately 1 mM compared to the recommended 20 mM). As validation of the methodology, two Gd(III)-complexes with known q and $GdCl_3$ were measured as controls (Table S2).

To improve accuracy, manual tuning and 90^o pulse calibration were performed on the instrument prior to acquisition. In addition, five NMR spectra were acquired for each sample using 64 scans per acquisition. The reference used for the controls was ^{17}O-enriched D_2O; the reference used for Gd(III) GO was GO in ^{17}O-enriched D_2O. MestReNova v7.0.2 (Mestrelab Research, Santiago de Compostela, Spain) was used for processing. Each FID was zero-filled to 16,384 points from the original 5,000 and smoothed with an exponential apodization function with 10 Hz line broadening. Each spectrum was then phased manually, and the chemical shift was obtained using Global Spectral Deconvolution (GSD) peak-picking set to 2 fitting cycles at high resolution. Fine phasing adjustments were performed by hand to ensure that the fitted peaks satisfactorily overlapped with the experimental data.

1.9 HYDRONMR simulation

The coordinates of the carbon atoms in two graphene sheets of 150×150 $Å^2$, spaced 3.6 Å apart, were generated and provided to the program HYDRONMR[21] to calculate the five components of the rotational correlation times (all in the range 380-440 ns) and the average reorientation correlation time. The latter result was about 400 ns.

1.10 Nuclear Magnetic Relaxation Dispersion (NMRD) experiment

Water proton longitudinal relaxation measurements were performed with a Stelar Spinmaster FFC-2000-1T fast field cycling relaxometer in the 0.01-40 MHz proton Larmor frequency range. Water proton relaxation rates were measured with an error smaller than 1%. Proton nuclear magnetic relaxation dispersion (NMRD) profiles were obtained from the field dependence of the solvent proton relaxation rates measured for the solution containing the Gd complex after subtraction of the diamagnetic contribution and normalization to 1 mM Gd(III) concentration. The diamagnetic contribution was determined by measuring the relaxation rates of graphene or graphene oxide (without Gd(III)) in similar concentration, and scaling to the same concentration present in the paramagnetic sample.

1.11 NMRD analysis

The Solomon-Bloembergen-Morgan (SBM) equations are often used to describe the relaxation profiles of water protons coordinated to paramagnetic metals (inner-sphere relaxation).[22-24] However, slow rotating systems containing a paramagnetic metal ion are known to display relaxation profiles that cannot be reproduced by the SBM equations if the electron energy levels of the paramagnetic metal ion are affected by static zero field splitting (ZFS).[25] A model has been developed by the Florence and Stockholm groups and successfully used to analyze these systems.[26-35] This model can take into account the effect of both static and transient ZFS on relaxation, provided that the system is in the slow motion limit (i.e., the rotational correlation time is larger than the electron relaxation time) and within the Redfield limit.[35] The static ZFS is introduced through the parameter D and the angle between the metal-water molecule direction and the z axis of the ZFS frame (θ). The other parameters affecting the relaxation profiles are those present in the SBM model, i.e. the metal-proton distance, r, the electron relaxation time ,T_{1e}, the reorientation correlation time, τ_R, and the water proton residence time, τ_M. The

electron relaxation has a field dependence which is described by the transient ZFS, Δ_t, and by a correlation time for electron relaxation, τ_v. A Lipari-Szabo order parameter (S^2) was introduced in the spectral density functions according to the model-free formalism,[36] with a correlation time τ_{fast} taking into accounts local motions occurring on a time scale much shorter than τ_R.[29] Contributions to relaxation from water molecules freely diffusing around the paramagnetic ion (outer-sphere relaxation) have also been considered according to the Freed model,[37,38] and described by two additional parameters: the distance of closest approach, d, of the water protons to the Gd(III) ion and the diffusion coefficient D_{diff}.

1.12 Inductively Coupled Plasmon-Mass Spectrometry (ICP-MS)

ICP-MS was performed on a Thermo Electron Corporation XSeries II ICP-MS with Thermo PlasmaLab software (Waltham, MA, USA). The instrument was calibrated by Fe and Gd quantitative standards of concentrations ranging from 1 to 250 ng/mL. Samples for analysis were incubated in ≥ 69% HNO_3 overnight at 60^{o}C, diluted to 3% v/v HNO_3 by milli-Q water, then filtered (polyacrylamide, 0.2 μm pore size) to remove any carbonaceous residues. All samples and standards were prepared with a multi-element internal standard (Bi, Ho, In, Li, Sc, Tb, and Y) at 5 ng/mL to allow for instrument drift compensation. Isotopes ^{57}Fe, ^{156}Gd, and ^{157}Gd were used to determine sample concentrations.

For validation, a second sample digestion protocol was followed and measurements were cross-validated by Inductively Coupled Plasmon-Optical Emission Spectroscopy (ICP-OES). To ensure that all Gd(III) ions were extracted from gadographenes for analysis, digestion using 3:2 HNO_3:H_2O_2 (30% w/w) was compared to using HNO_3 alone. In addition, measurements performed on a Varian Vista MPX ICP-OES (Palo Alto, CA, USA) were compared to readings from ICP-MS to ensure accuracy of the concentration measurements. Emission wavelengths 234.4 nm, 238.2 nm, and 259.9 nm were used for Fe measurement while 335.9 nm, 336.2 nm, and 342.2 nm were used for Gd measurement. Consistent

results for Gd were obtained regardless of the digestion protocol or the measurement technique used (Table S7).

1.13 Simulation of relaxivities at 60 MHz as a function of τ_R and τ_M

Simulation of inner-sphere r_1, r_2, and r_2/r_1 ratio at 60 MHz was performed using modified SBM equations (eq [S17]-[S27])[17,39] in Maple V14 (Waterloo, ON, Canada). [Gd] was set to 1 mM, and R_1 ($1/T_1$) and R_2 ($1/T_2$) were calculated across different values of τ_R and τ_M.

The total relaxation rates of water protons in the presence of Gd(III) are described by

$$\frac{1}{T_1} = \frac{q[Gd]}{[H_2O]}\left(\frac{1}{T_{1m}+\tau_m}\right) \quad [S17]$$

$$\frac{1}{T_2} = \frac{q[Gd]}{[H_2O]}\frac{1}{\tau_m}\left(\frac{T_{2m}^{-2}+\tau_m^{-1}T_{2m}^{-1}+\Delta\omega_m^2}{\left(\tau_m^{-1}+T_{2m}^{-1}\right)^2+\Delta\omega_m^2}\right) \quad [S18]$$

q is the hydration number, T_{1m} and T_{2m} are, respectively, the longitudinal and transverse proton relaxation times of Gd(III)-coordinated water, $\Delta\omega_m$ is the chemical shift difference between bound and bulk water proton, and τ_M is the residence lifetime of inner-sphere water.

Relaxation of inner-sphere water can be separated into that resulting from dipole-dipole interactions and that resulting from scalar interactions,

$$\frac{1}{T_{im}} = \frac{1}{T_i^{DD}} + \frac{1}{T_i^{SC}} \quad i = 1,2 \quad [S19]$$

$$\frac{1}{T_1^{DD}} = \frac{2}{15}\left(\frac{\mu_o}{4\pi}\right)^2 \frac{\gamma_H^2\gamma_S^2\hbar^2 J(J+1)}{r^6}\left(7\frac{\tau_{c2}}{1+\omega_S^2\tau_{c2}^2} + 3\frac{\tau_{c1}}{1+\omega_H^2\tau_{c1}^2}\right) \quad [S20]$$

$$\frac{1}{T_1^{SC}} = \frac{2J(J+1)}{3}\left(\frac{A}{\hbar}\right)^2\left(\frac{\tau_{e2}}{1+\omega_S^2\tau_{e2}^2}\right) \quad [S21]$$

$$\frac{1}{T_2^{DD}} = \frac{1}{15}\left(\frac{\mu_o}{4\pi}\right)^2 \frac{\gamma_H^2\gamma_S^2\hbar^2 J(J+1)}{r^6}\left(13\frac{\tau_{c2}}{1+\omega_S^2\tau_{c2}^2} + 3\frac{\tau_{c1}}{1+\omega_H^2\tau_{c1}^2} + 4\tau_{c1}\right) \quad [S22]$$

$$\frac{1}{T_2^{SC}} = \frac{J(J+1)}{3}\left(\frac{A}{\hbar}\right)^2\left(\frac{\tau_{e2}}{1+\omega_S^2\tau_{e2}^2} + \tau_{e1}\right) \quad [S23]$$

$$\frac{1}{\tau_{ci}} = \frac{1}{\tau_R} + \frac{1}{\tau_m} + \frac{1}{T_{ie}} \quad i = 1,2 \quad [S24]$$

$$\frac{1}{\tau_{ei}} = \frac{1}{\tau_m} + \frac{1}{T_{ie}} \quad i = 1,2 \quad [S25]$$

μ_o is the permeability of free space, Υ_H and Υ_s are the proton and electron gyromagnetic ratios, $\hbar$ is the Planck constant, J = S = 7/2 for Gd(III), r is the proton-Gd(III) distance, ω_s and ω_H are the electron and proton precession angular frequencies, $A/\hbar$ is the hyperfine coupling constant between Gd(III) and the coordinated water proton, τ_R is the rotational correlation time, and T_{1e} and T_{2e} are the longitudinal and transverse electronic relaxation times, respectively.

The chemical shift of inner-sphere water with respect to the bulk water can be separated into the diamagnetic, the contact, and the pseudocontact components.[20,39] For Gd(III), the contact component dominates.[20]

$$\Delta\omega_m = \Delta\omega_m^{dia} + \Delta\omega_m^{con} + \Delta\omega_m^{pseudo} \approx \Delta\omega_m^{con} \quad [S26]$$

$$\Delta\omega_m^{con} = \frac{g(g-1)J(J+1)\mu_B B_0}{3k_B T}\frac{A}{\hbar} \quad [S27]$$

B_0 is the main magnetic field, g is the Landé g-factor, μ_B is the Bohr magneton, k_B is the Boltzmann constant, and T is the absolute temperature. For simulation, T = 310 K, B_0 = 1.41 T (60 MHz) or 0.47 T (20 MHz), r = 3.05 Å, q = 1, $A/\hbar = 1 \times 10^6$ rads·s^{-1}, $T_{1e} = T_{2e}$ = 10 ns. r was chosen from the lowest values tabulated in a review by Caravan, et al., T_{1e} and T_{2e} were fixed based on measurements at 0.35 T with a quoted range of 1-5 ns, and $A/\hbar$ was chosen to be a quarter of the Gd-O coupling constant. The choice of $A/\hbar$ has relatively low confidence compared to the other parameters.

2. Supplementary Tables

Table S1. Comprehensive list of gadographene samples

	Sonication					r_1 (mM $Gd^{-1}s^{-1}$)			r_2 (mM $Gd^{-1}s^{-1}$)				
Sample	Power (W)	Time (h)	[Gd] (μM)	[Fe] (μM)	Loading ($Gd/10^4C$)	Fresh	Corr-ected[a]	Aged[b]	Fresh	Corr-ected[a]	Aged[b]	Contami-nation[c]	Figure
Carbon Nanomaterials													
Graphene 2%SC[d]	55	16	< 0.1	76								Na,Ti,Zn Only	
Graphene Oxide (GO)													
Batch 1 (H_2O)[e]			< 0.1	23								+Cr,Mn -Ti	
Batch 2 (D_2O)			< 0.1	30								+Ca,Br -Ba	
Reduced GO (rGO)			< 0.1	< 10								Na,Ti,Mn,Zn Only	
Graphite Flake												+Mn,Sr,Ce	
Ionic Gadographenes													
Gd(III) Graphene 2%SC													
Preparation 1	40	0.75	31	81	11.5	49	46	-5%	96	78	+3%		1,2A-C,4
Preparation 2	55	1	38	89	8.7	54	51	-37%	99	83	-26%		1,2A-C
Preparation 3	70	1	28	67	6.8	57	54	-45%	104	88	-33%		1,2A-C
Preparation 4A	55	16	25	26	6.2	60	59	-33%	101	94	-24%	-Al	1,2A-C
Preparation 4B	55	16	55	39	12.5	86	85	-23%	146	141	-20%	-Al	
Gd(III) Graphene 2%PL													
Preparation 1	40	0.75	44	141	10.8	35	30	-7%	69	48	-8%		1,2A-C,4
Preparation 2A	55	1	47	118	9.2	34	30	-5%	64	48	+2%		1,2A-C, S4
Preparation 2B	55	1	29	47	8.3	28	26	N/M	50	39	N/M	+Mo	1,2A,C,S4
Preparation 2C	55	1	29	55	7.6	29	26	N/M	53	40	N/M	+Mo	1,2A,C,S4
Preparation 3	70	1	43	112	7.0	29	25	-9%	57	40	-1%		1,2A-C
Preparation 4A	55	16	17	27	4.9	23	21	-11%	38	28	-6%	-Al	1,2A-C,S4
Preparation 4B	55	16	20	19	3.2	22	21	N/M	34	28	N/M	-Na,Mg,Al	1,2A,C,S4
Preparation 4C	55	16	22	31	3.3	22	20	N/M	34	24	N/M	+Mo -Al	1,2A,C,S4
Gd(III) Graphene Oxide													
Preparation 1A (H_2O)			175	< 10	71.9	78	78[f]	+8%	104	103[f]	+13%	-Al	1,2C,3,4,S4
Preparation 1B (D_2O)			799	33	51.5	85	85[f]	N/M	115	115[f]	N/M	+Br -Al,I,Ba	1,2C,3,S4
Complexed Gadographenes													
Gd(III)-DO3A Graphene 2%SC	55	16	15	10	21.4	25	24		47	42		-Al,Ti,I,Ba	1,2C
Gd(III)-DO3A Graphene 2%PL													
Preparation 1A	40	0.75	95	15	46.7	12	12		25	24		-Al,Ti,I,Ba	1,2C
Preparation 1B	55	1	43	9	12.1	14	14		27	26		-Al,I,Ba	1,2C
Preparation 1C	55	1	61	N/M	27.6	17		-8%	29		-5%	-I,Ba	1,2C
Gd(III)-DO3A GO													
Graphene Oxide			404	N/M	120	49			86			Na Only	1,2C,5
Reduced GO			251	N/M	73.5	63			102			Na Only	1,2C,5
Gd(III)-DTPA GO													
Graphene Oxide			315	N/M	88.9	28			46			Na Only	1,2C,5
Reduced GO			242	N/M	72.5	32			51			Na Only	1,2C,5
Others[g]													
Fe Graphene 2%PL													
Preparation 1A	55	1	< 0.1	93	24.8	0.9			3.6			+Mo -Na,Mg,Al	S4
Preparation 1B	55	1	< 0.1	77	22.3	1.0			4.4			+Mo -Al	S4
Preparation 2A	55	16	< 0.1	37	6.5	1.1			2.4			-Al,Ba	S4
Preparation 2B	55	16	< 0.1	36	6.2	1.1			2.3			-Al,Ti	S4
Fe Graphene Oxide			< 0.1	872	215	6.2			7.1			+Sn -Al	S4
Tb Graphene Oxide			1054	N/M	193	0.3			1.7			N/M	S4

[a] Relaxivity was corrected for Fe unless otherwise noted using eq [S1]. Figures in the main text report the corrected relaxivities where available.
[b] Re-measured prior to NMRD acquisition using the one-point method. Ages range from several months to more than a year post-preparation.
[c] Based on ICP-MS survey scan. All samples contain measurable amounts of Na, Mg, Al, K, Ti, Zn, I, and Ba unless otherwise noted.
[d] relaxivity of this sample on a per Fe basis was used as the correction factor for all other samples utilizing graphene 2%SC or 2%PL.
[e] relaxivity of this sample on a per C basis was used as the correction factor for all other samples utilizing GO.
[f] Relaxivity corrected for carbon; [g] Concentration, loading, and relaxivity based on Fe or Tb instead of Gd.

In general, the relaxivities of gadographenes are stable over time, changing by < ∼10% after several months to more than a year of storage when the measurement error of the single-point method is taken into consideration. However, Gd(III) Graphene 2%PL Preparations 2-4 experienced significant aging effects. Gd(III) Graphene 2%PL 4B has exceptionally high relaxivity and is considered an outlier.

Table S2. q and χ of gadographenes and controls

Sample	[Gd] (mM)	Lock	$\delta^{17}O$ (ppm)	δ_{obs} (ppm)	q	δ_χ (ppm)	μ_{eff} (μ_B)
Measured at 296 K							
D_2O		✓	22.9143 ± 0.0084				
Gd(III)-HP-DO3A	2.69	✓	22.8510 ± 0.0178 23.1710 ± 0.0137	-0.0633 ± 0.0197	0.5 ± 0.2 (1.3 ± 0.1)[a]	0.3200 ± 0.0225	8.2 ± 0.3 (7.9)[b]
Gd(III)-DO3A	3.23	✓	22.7744 ± 0.0289 23.0669 ± 0.0338	-0.1399 ± 0.0301	0.9 ± 0.2 (1.8 ± 0.2)[a]	0.2925 ± 0.0445	7.2 ± 0.5 (7.9)[b]
$GdCl_3$	0.67	✓	22.6176 ± 0.0092 22.7201 ± 0.0094	-0.2967 ± 0.0125	9.5 ± 0.4 (8 - 9)[a]	0.1025 ± 0.0132	9.3 ± 0.6 (7.9)[b]
GO		✓	23.1471 ± 0.0109				
Gd(III) GO	0.80	✓	22.9663 ± 0.0101 23.0599 ± 0.0178	-0.1808 ± 0.0149	4.9 ± 0.4	0.0936 ± 0.0205	8.2 ± 0.9 (7.9)[b]
Measured at 353 K							
D_2O		✓	20.8649 ± 0.0049				
Gd(III)-HP-DO3A	2.69	✓	20.7682 ± 0.0074 20.9987 ± 0.0081	-0.0967 ± 0.0089	0.9 ± 0.1 (1.3 ± 0.1)[a]	0.2305 ± 0.0110	7.6 ± 0.2 (7.9)[b]
Gd(III)-DO3A	3.23	✓	20.6134 ± 0.0095 20.8847 ± 0.0079	-0.2516 ± 0.0107	2.0 ± 0.1 (1.8 ± 0.2)[a]	0.2713 ± 0.0124	7.6 ± 0.2 (7.9)[b]
$GdCl_3$	0.67	✓	20.6025 ± 0.0043 20.6550 ± 0.0036	-0.2624 ± 0.0065	10.1 ± 0.3 (8 - 9)[a]	0.0525 ± 0.0056	7.3 ± 0.4 (7.9)[b]
GO		✓	21.0532 ± 0.0030				
Gd(III) GO	0.80	✓	20.9027 ± 0.0079 20.9653 ± 0.0033	-0.1505 ± 0.0085	4.9 ± 0.3	0.0626 ± 0.0086	7.3 ± 0.5 (7.9)[b]

± denotes standard deviation of five acquisitions following the appropriate error propagation methods

Numbers in parentheses are literature values ([a] ref 9; [b] ref 40); [Gd] was measured by ICP-MS

δ_{obs} was obtained by subtracting the appropriate reference from the locked $\delta^{17}O$; D_2O was used as the reference for Gd(III)-HP-DO3A, Gd(III)-DO3A, and $GdCl_3$; GO was used as the reference for Gd(III) GO

q was obtained from δ_{obs} using eq [S15]

δ_χ was obtained from the difference of the locked and unlocked $\delta^{17}O$

χ was not directly calculated but inferred from the effective magnetic moment μ_{eff} calculated using eq [S16]

Processing of 296 K and 353 K data was performed in VnmrJ and MestReNova, respectively

Gd(III) GO Preparation 1B and GO Batch 2 (Table S1) were used for this study. The measurement of q is inaccurate for Gd(III)-HP-DO3A and Gd(III)-DO3A at 296 K because water exchange is slower than the NMR timescale at this temperature. In contrast, the measured q of $GdCl_3$ and Gd(III) GO are consistent across the two different temperatures because the water exchange for these samples are two orders of magnitude faster than those of the Gd(III)-complexes. All measured μ_{eff} roughly agree with the theoretical value.

Table S3. Full table of fitted NMRD parameters for Gd(III) GO

Measured values		
q		5
μ_{eff} (μ_B)		7.3
r_2 ($mM^{-1}s^{-1}$)	310K	116
Literature values		
r (Å)		3.1
d (Å)		3.8
D_{diff} (cm^2/s)	298K	2.3×10^{-5}
	310K	3.3×10^{-5}

Fitted values		
	Modified Florence 298K/310K	with local motions 298K/310K
τ_R (ns)	≥ 1000	≥ 1000
S^2	N/A	0.43
τ_{fast} (ps)	N/A	120/100
τ_M (ns)	0.74/0.64	1.8/1.6
Δ_t (cm^{-1})	0.0253	0.0218
τ_v (ps)	20.8/20.2	25/24
D_{ZFS} (cm^{-1})	0.047	0.05
Θ (°)	43	38
Predicted r_2 ($mM^{-1}s^{-1}$)	127/111	128/116

Δ_t = transient ZFS, τ_v = electron correlation time

D_{ZFS} = axial static ZFS parameter, Θ = polar angle between principle static ZFS axis and dipole-dipole axis of the proton and electron spin

Table S4. Full table of fitted NMRD Parameters for Gd(III) Graphenes

Fixed values			
r (Å)	3.1	τ_R (ns)	≥ 1000
d (Å)	3.8	τ_M (ns)	1.6
D_{diff} (cm^2/s)	3.3×10^{-5}		

Fitted values when q is fixed at 5			
	Gd(III) Graphene Oxide	Gd(III) Graphene 2%SC	Gd(III) Graphene 2%PL
S^2	0.43	0.22	0.145
τ_{fast} (ps)	100	12	15
Δ_t (cm^{-1})	0.0218	0.0163	0.0204
τ_v (ps)	24	28	20
D_{ZFS} (cm^{-1})	0.05	0.045	0.052
Θ (°)	38	40	38

Fitted values when τ_{fast} is fixed at 100 ps			
	Gd(III) Graphene Oxide	Gd(III) Graphene 2%SC	Gd(III) Graphene 2%PL
q	5	3	2
S^2	0.43	0.36	0.34
Δ_t (cm^{-1})	0.0218	0.019	0.019
τ_v (ps)	24	24	20
D_{ZFS} (cm^{-1})	0.05	0.05	0.05
Θ (°)	38	43	42

Table S5. Full table of fitted NMRD parameters for Gd(III)-complex GO

	S^2	τ_{fast} (ns)	Δ_t (cm^{-1})	τ_v (ps)	D_{ZFS} (cm^{-1})	Θ (°)	τ_M (ns)	q
Gd(III)-DO3A-rGO	0	1.55	0.018	19	0.045	53	77	2
Gd(III)-DO3A-GO	.06	1.05	0.019	20	0.045	53	77	2
Gd(III)-DTPA-rGO	0	1.65	0.016	23	0.05	50	130	1
Gd(III)-DTPA-GO	0	1.44	0.016	23	0.05	48	130	1

Table S6. Relaxation times of controls at 60 MHz and 310 K

Sample	T_1 (ms)	T_2 (ms)
2% Sodium Cholate	3740	2439
2% Pluronic F108	3790	2918
0.5 mg/mL Graphene 2% SC	2680	1205
0.5 mg/mL Graphene 2% PL	2821	1192
0.5 mg/mL Graphene Oxide	2851	1454
Water	3860	2603

Table S7. Validation of [Fe] and [Gd] measurement accuracy by ICP

	HNO_3 ICP-MS		3:2 HNO_3:H_2O_2 ICP-MS		HNO_3 ICP-OES	
Sample	**[Gd] (μM)**	**[Fe] (μM)**	**[Gd] (uM)**	**[Fe] (μM)**	**[Gd] (μM)**	**[Fe] (μM)**
Gd(III) Graphene 2%SC						
Preparation 1	31	81			33	128
Preparation 2	38	89			40	95
Preparation 3	28	67			31	50
Preparation 4A	25	26			26	< 45
Preparation 4B	55 ± 2	37 ± 11	55 ± 1	40 ± 20		
Gd(III) Graphene 2%PL						
Preparation 2A	47	124	47	113		
Preparation 2C	29	57	28	54		
Preparation 3	43	106	43	118		
Preparation 4A	17	31	17	23		
Preparation 4C	22	31	23	70		
Fe Graphene 2%PL						
Preparation 1B		78		75		
Preparation 2B		36		179		

± denotes standard deviation over several analysis sample preparations

Consistent [Gd] measurements were obtained regardless of the sample digestion method or the ICP technique used. However, [Fe] differed by more than 20% across different measurements in five out of the twelve instances, indicating the larger errors associated with [Fe] compared to [Gd].

3. Supplementary Figures

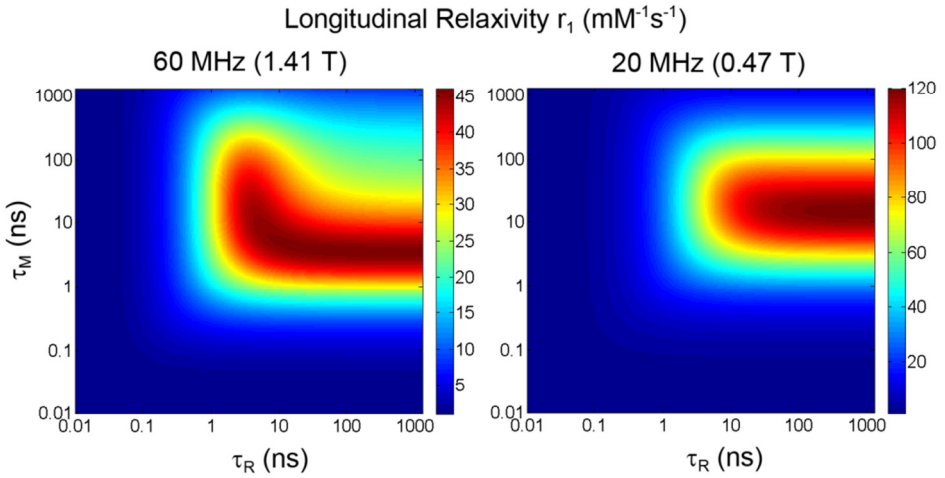

Figure S1. Maximum longitudinal relaxivity (r_1) for a Gd(III)-based agent at 60 MHz and 20 MHz with q = 1. The theoretical maximum is approximately 45 $mM^{-1}s^{-1}$ and 120 $mM^{-1}s^{-1}$ for 60 MHz and 20 MHz, respectively. These maxima occur when τ_R > 10 ns and τ_M is optimized to approximately 10 ns. Refer to Materials and methods for details of the simulation.

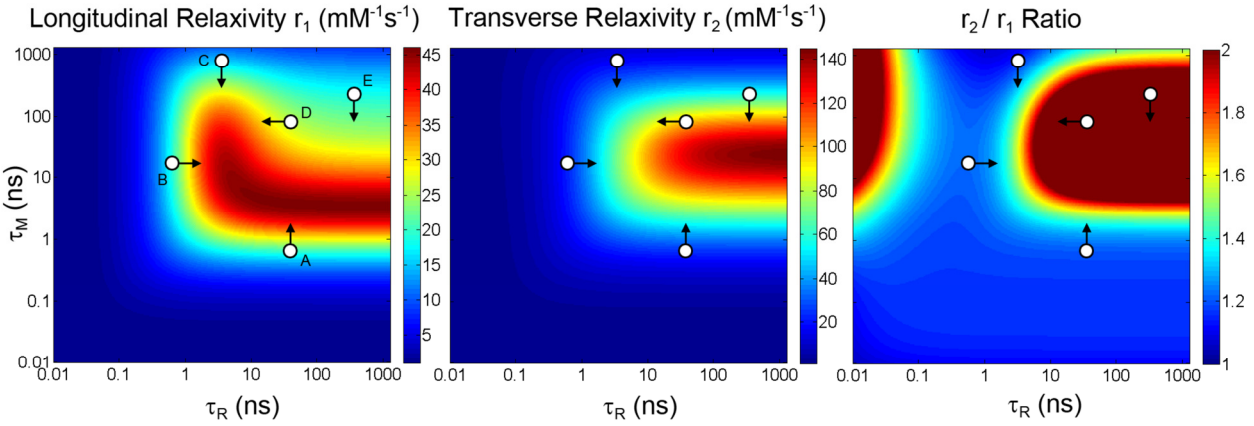

Figure S2. Theoretical analysis of r_2/r_1 ratio at 60 MHz. In different regimes of τ_R and τ_M, r_1, r_2, and r_2/r_1 ratio trends differently with the two parameters. In regime A (τ_R > 1 ns, τ_M < 1 ns), r_1 increases, r_2 increases, and r_2/r_1 increases with increasing τ_M, this is part of the fast exchange regime. In regime B (τ_R < 1 ns, τ_M > 1 ns), r_1 increases, r_2 increases, and r_2/r_1 increases with increasing τ_R, this is the typical regime for small molecule Gd(III)-complexes. In regime C (1 ns < τ_R < 10 ns, τ_M > 10 ns), r_1 increases, r_2 increases, and r_2/r_1 increases with decreasing τ_M, this is part of the slow exchange regime. In regime D (τ_R > 10 ns, τ_M > 10 ns), r_1 increases, r_2 decreases, and r_2/r_1 decreases with decreasing τ_R, this is the only regime that explains the r_1 trend of Gd(III) Graphene 2%SC, but it fails to rationalize the observed r_2 trend. In the same regime (E), r_1 increases, r_2 increases, and r_2/r_1 increases with decreasing τ_M. This regime is difficult to access because few agents achieve a τ_R > 10 ns given the rotational degree of freedom in sigma bonds. The τ_R and τ_M of gadographenes are both likely to be above 1 ns given that their r_2/r_1 > 1.2. The case of τ_R < 0.1 ns is not considered because it is not physically plausible. Refer to Materials and methods for details of the simulation.

Graphene Oxide

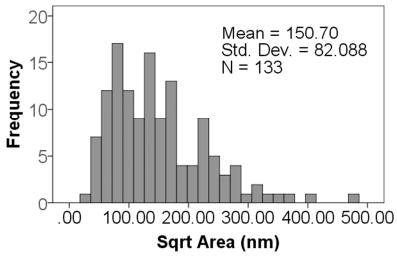

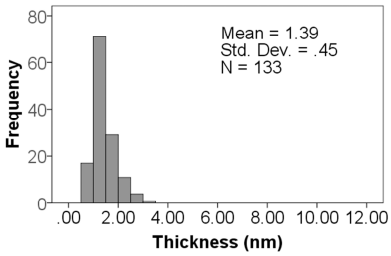

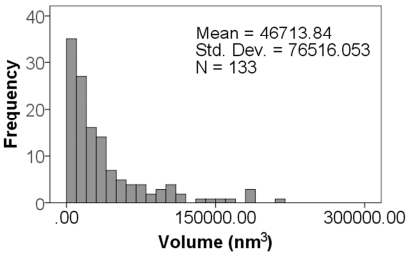

Gd(III) Graphene 2%SC Preparation 1 30 W-h Sonication

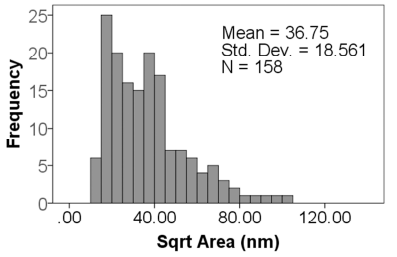

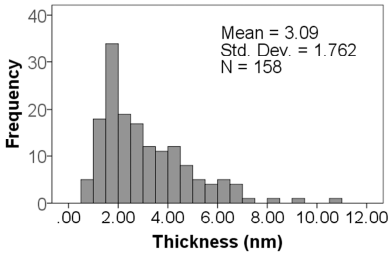

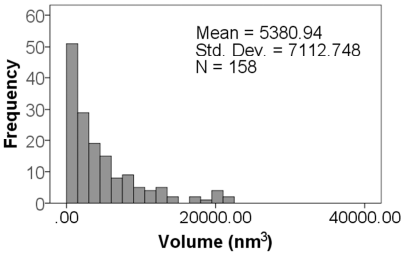

Gd(III) Graphene 2%SC Preparation 2 55 W-h Sonication

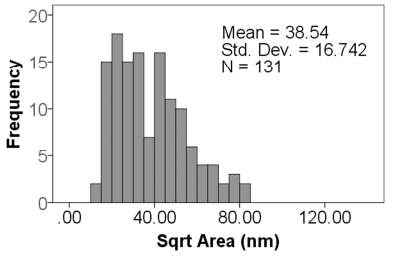

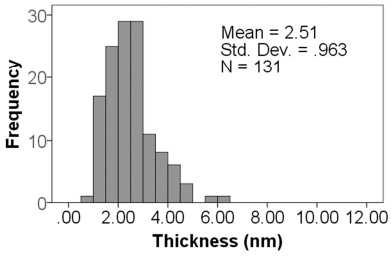

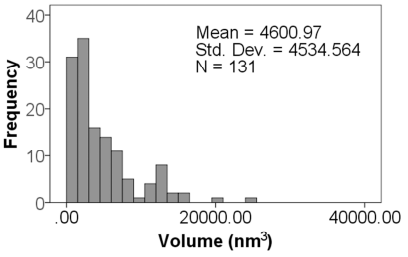

Gd(III) Graphene 2%SC Preparation 3 70 W-h Sonication

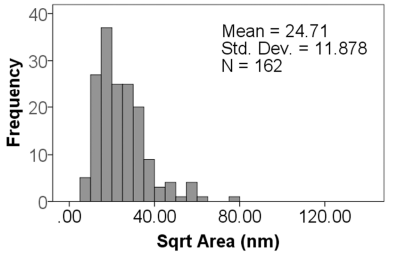

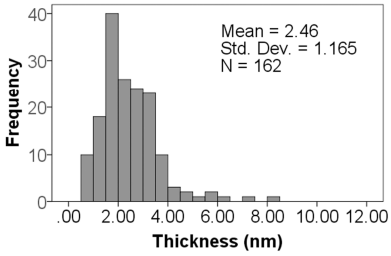

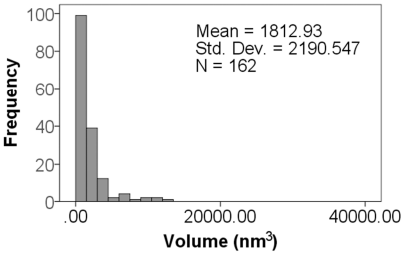

Gd(III) Graphene 2%SC Preparation 4A 880 W-h Sonication

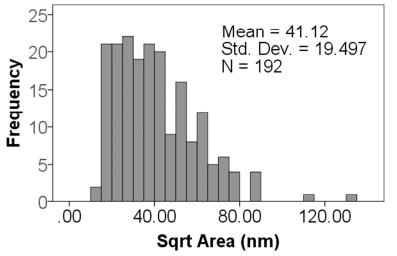

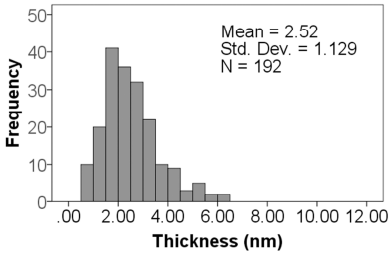

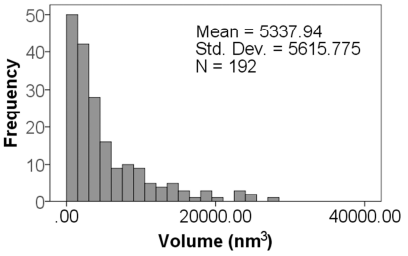

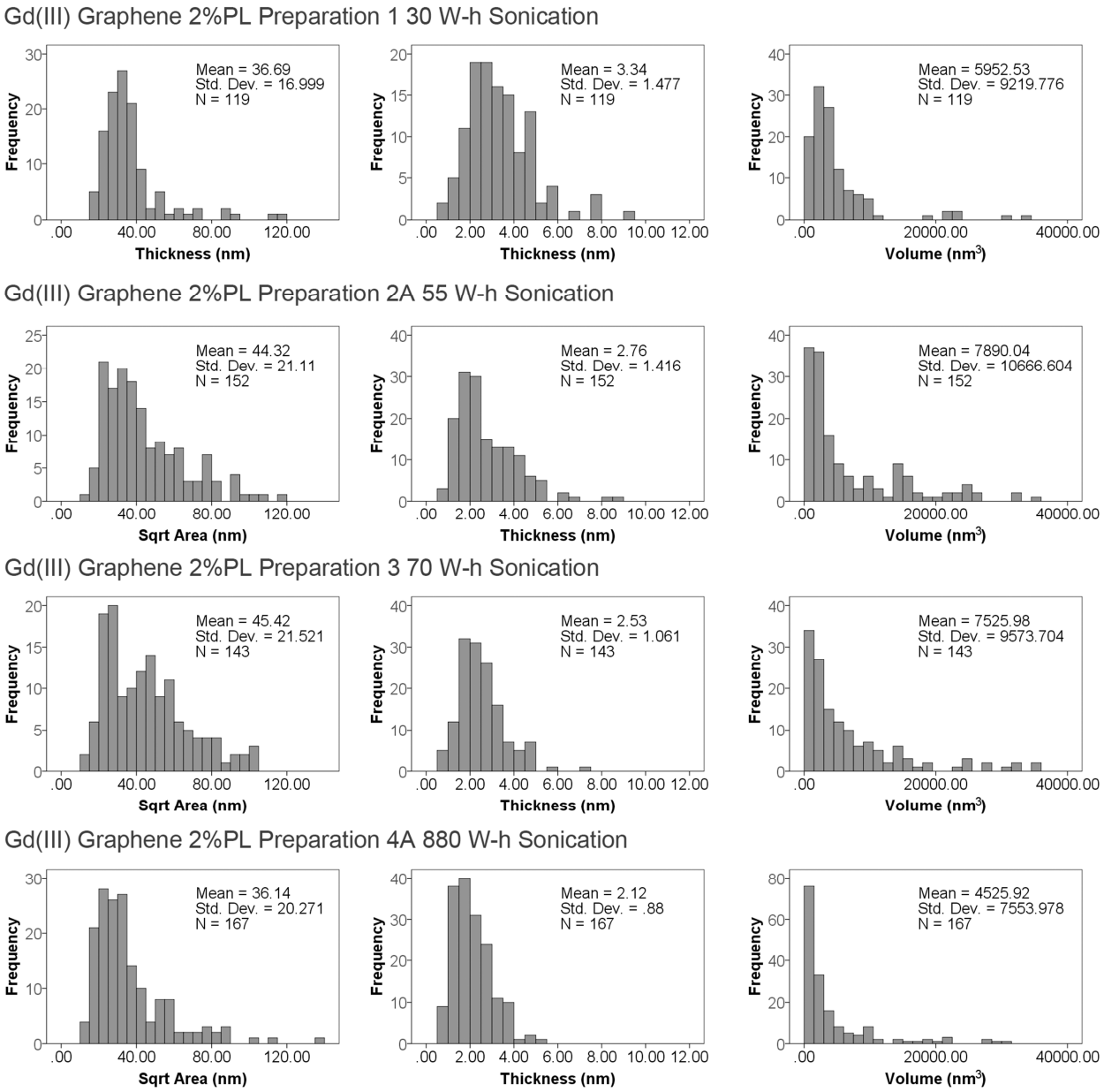

Figure S3. AFM size distributions. Histograms of square root area, thickness, and volume of gadographenes as measured by Atomic Force Microscopy. The Gaussian mean and standard deviation was calculated for each distribution. Thickness was observed to decrease with sonication. The noise in the square root area and volume were too large for reliable comparisons across samples. Thus, their correlation to Gd(III) Graphene relaxivity was not analyzed.

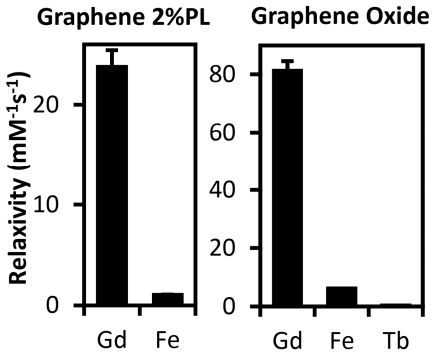

Figure S4. Additional relaxivity trends in gadographene. The r_1 relaxivity of gadographene is diminished when Gd(III) is replaced with iron or terbium, and enhanced when GO is used as a scaffold compared to graphene. This result suggests that any potential magnetic coupling between Gd(III) and the carbon backbone is not generalizable to other metal ions and that graphene itinerant electrons are not the primary determinant of gadographene relaxivity.

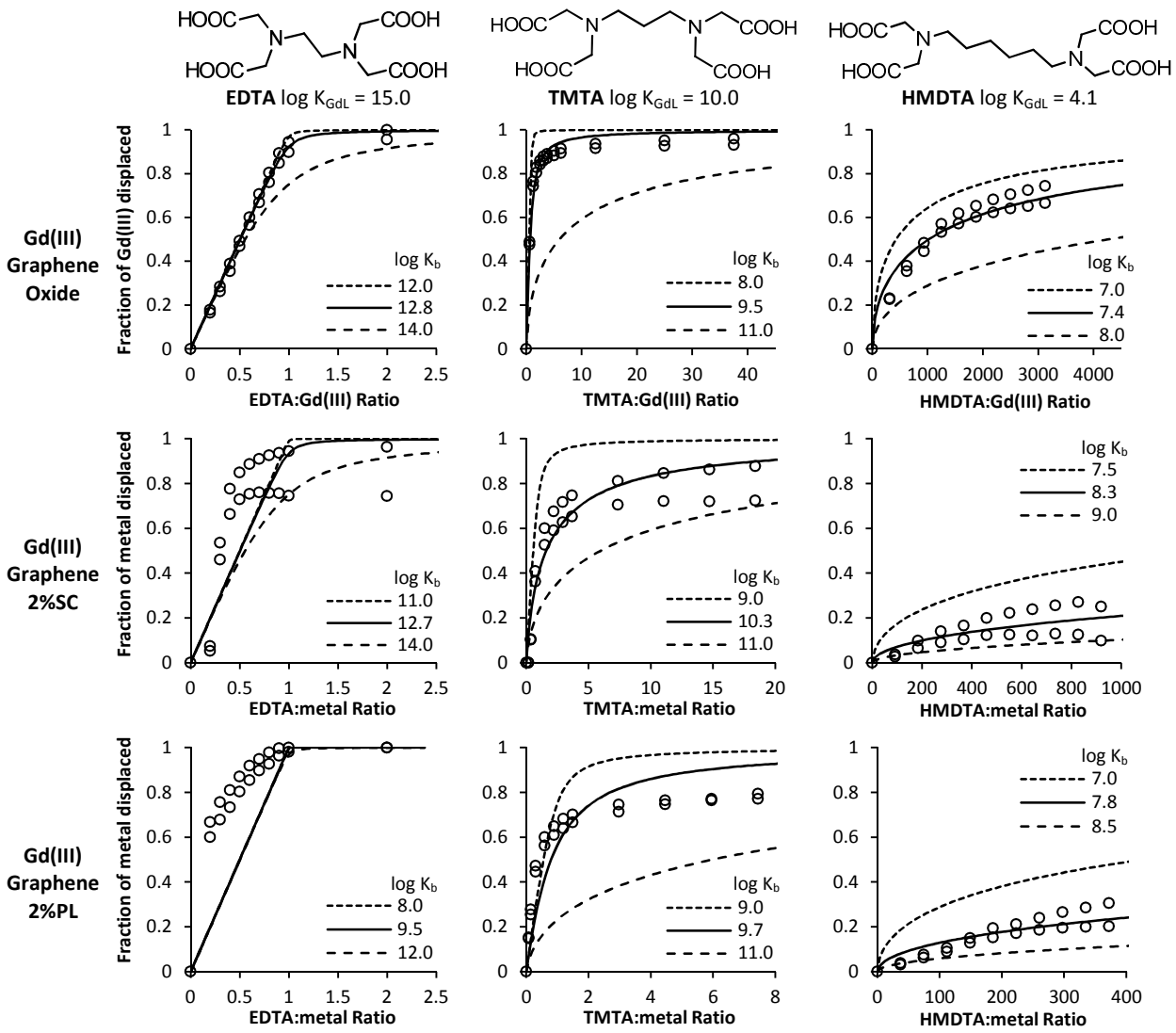

Estimates of log K_b

	EDTA	TMTA	HMDTA	CO_3^{2-}
Gd(III) GO	< 12.8	9.5	7.4	11.3
Gd(III) Graphene 2% SC	< 12.7	10.3	8.3	11.3
Gd(III) Graphene 2% PL	< 9.5	9.7	7.8	

Gd(III)-EDTA and $Gd_2(CO_3)_3$ Relaxivity in HEPES

	r_1 ($mM^{-1}s^{-1}$)	r_2 ($mM^{-1}s^{-1}$)
$GdCl_3$	6.8 ± 1.1	9.4 ± 2.0
+ > 1 eq EDTA	5.0 ± 0.2	5.2 ± 0.6
+ > 200 eq $NaHCO_3$	3.5 ± 0.5	6.3 ± 0.9

Figure S5. Binding constants (K_b) of Gd(III) in various gadographene materials. Each gadographene was challenged with EDTA, TMTA, HMDTA, and $NaHCO_3$ to obtain four independent estimates of K_b. Results show that the log K_b of Gd(III) GO, Gd(III) Graphene 2%SC, and Gd(III) Graphene 2%PL are comparable, in the range of 8-10. [Fe] and [Gd] were analyzed together as [metal] in the graphene samples; the GO sample contained no measurable amount of iron. Data deviated more from the model in graphene compared to GO due to complications introduced by iron and possibly by surfactants. Dashed fits give indication of the precision of the obtained K_b. Two points are available at each ligand:metal ratio because displacement fraction was estimated by both T_1 and T_2 measurements. The relaxivities of Gd(III)-EDTA and $Gd_2(CO_3)_3$ were used in the calculation of displacement fraction. Gd(III) GO 1A, Gd(III) Graphene 2%SC 3, and Gd(III) Graphene 2%PL 1 were studied (Table S1). ± represent standard deviation.

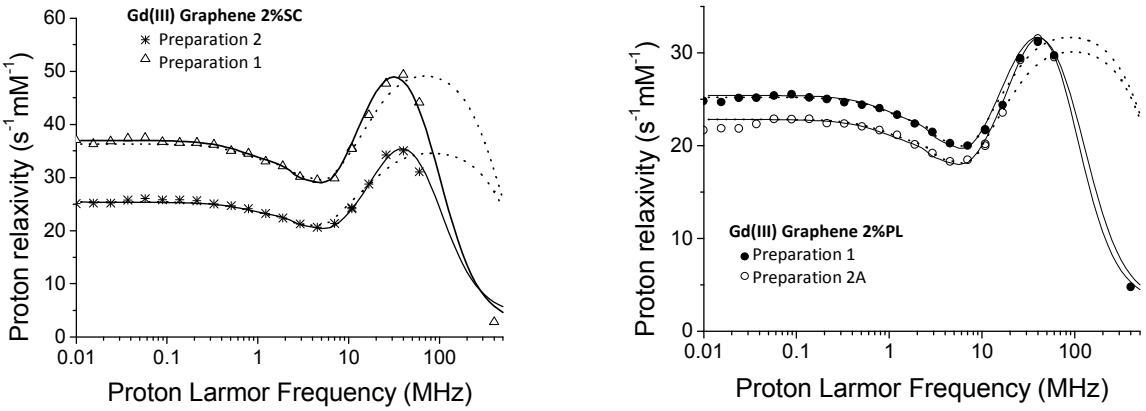

	S^2	$(\tau_R^{-1}+\tau_M^{-1})^{-1}$ (ns)	$T_{1e}^{100\ kHz}$ (ps)	Δ_t (cm^{-1})	τ_v (ps)	D_{ZFS} (cm^{-1})	Θ (°)
Gd(III) Graphene 2%SC							
Preparation 1							
Rigid model	N/A	0.32	88	0.032	26	0.045	42
With local motions	0.22	N/A	315	0.0163	28	0.045	40
Preparation 2							
Rigid model	N/A	0.22	58	0.040	26	0.043	40
With local motions	0.16	N/A	257	0.0195	24	0.050	40
Gd(III) Graphene 2%PL							
Preparation 1							
Rigid model	N/A	0.20	35	0.0475	30	0.055	30
With local motions	0.145	N/A	282	0.0204	20	0.052	38
Preparation 2A							
Rigid model	N/A	0.19	33	0.0506	28	0.055	30
With local motions	0.15	N/A	274	0.0218	18	0.050	43

Fixed values for rigid model: q=5, r =3.1 Å, d=3.8 Å, $D=3.3\times10^{-5}$ cm^2/s

Fixed values with local motions: q=5, r =3.1 Å, d=3.8 Å, $D=3.3\times10^{-5}$ cm^2/s, $\tau_R \geq 1000$ ns, $\tau_M=1.6$ ns, $\tau_{fast}=12$ ps (SC) / 15 ps (PL)

Figure S6. Comparison of Gd(III) Graphene NMRD fitting with and without inclusion of local motion. Similar to the findings in Gd(III) Graphene Oxide, significantly better NMRD fits were found for Gd(III) Graphene 2%SC and 2%PL when local motions are taken into account (solid lines −) compared to when a rigid model (dotted lines ···) is assumed. Therefore, fast local motions are likely an important feature of ionic gadographenes. It is worth noting that if $\tau_M > 500$ ns, reasonable fits can be found with the rigid model. This scenario appears less plausible than the scenario with fast local motion due to 1) the result of the temperature-dependent NMRD experiment (Figure S8), 2) the similar binding constant between Gd(III) GO and Gd(III) Graphene (Figure S5), indicating similar Gd(III) microenvironments, and 3) the large magnitude of τ_M. Nevertheless, it remains a possibility for Gd(III) Graphene 2%SC and 2%PL.

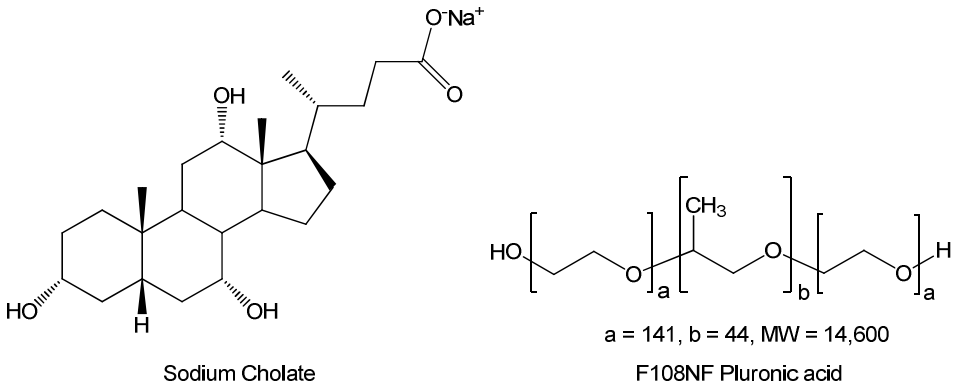

Figure S7. Chemical structures of sodium cholate and F108NF pluronic acid.

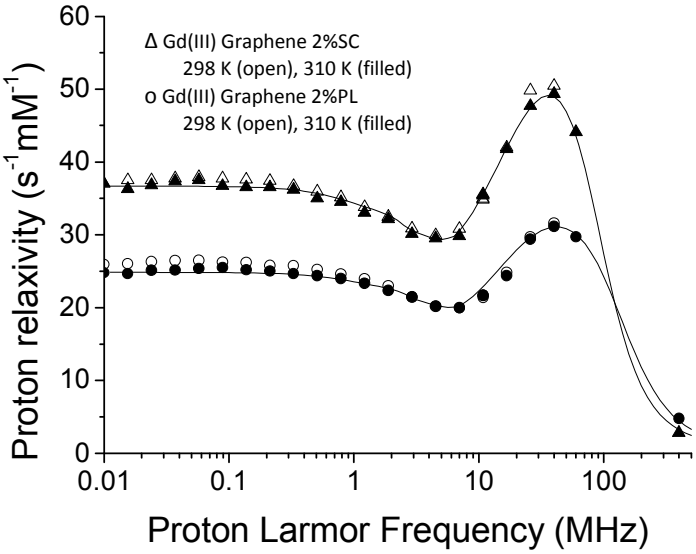

Figure S8. Temperature-dependent NMRD of Gd(III) Graphene for τ_M elucidation. Similar to Gd(III) Graphene Oxide, lower relaxivities were measured at 310 K than at 298 K for Gd(III) Graphene. However, the difference is of insufficient magnitude to conclude that τ_M is in the fast exchange regime by quantitative analysis. The samples measured were Gd(III) Graphene 2%SC Preparation 1 and Gd(III) Graphene 2%PL Preparation 1 (Table S1).

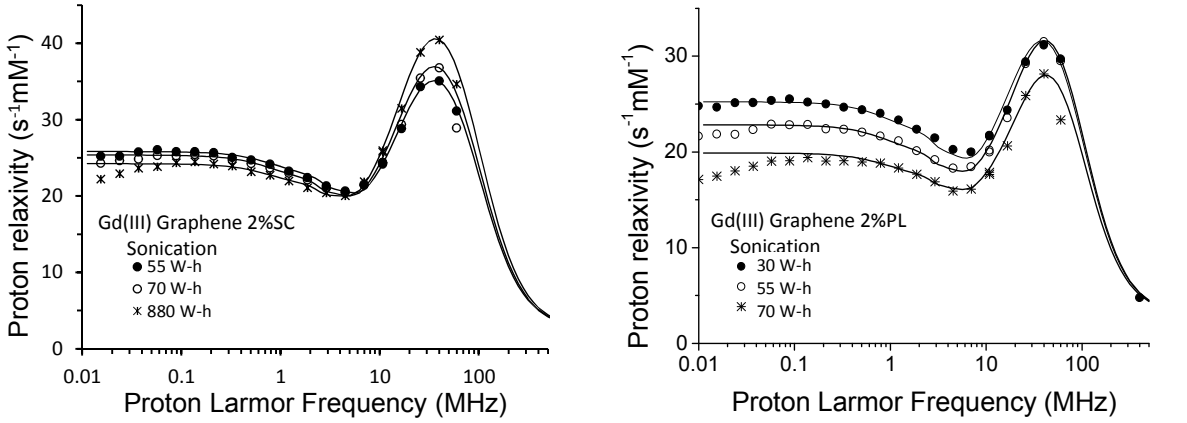

	Gd(III) Graphene 2%SC			Gd(III) Graphene 2%PL		
Sonication	55 W-h	70 W-h	880 W-h	30 W-h	55 W-h	70 W-h
S^2	0.16	0.17	0.19	0.145	0.15	0.132
$T_{1e}^{100\ kHz}$(ps)	257	257	197	282	274	246
Δ_t (cm^{-1})	0.0195	0.0195	0.021	0.0204	0.0218	0.023
τ_v (ps)	24	24	27	20	18	18
D_{ZFS} (cm^{-1})	0.05	0.045	0.045	0.052	0.05	0.05
Θ (^{o})	40	41	44	38	43	45
τ_{fast} (ps) (fixed)	12	12	12	15	15	15
Predicted r_2 ($mM^{-1}s^{-1}$)	43	46	51	40	40	35
Measured r_2 ($mM^{-1}s^{-1}$)	60	54	56	55	53	39

Fixed values: q=5, r =3.1 Å, d=3.8 Å, D=3.3 × 10^{-5} cm^2/s, $\tau_R \geq 1000$ ns, τ_M=1.6 ns

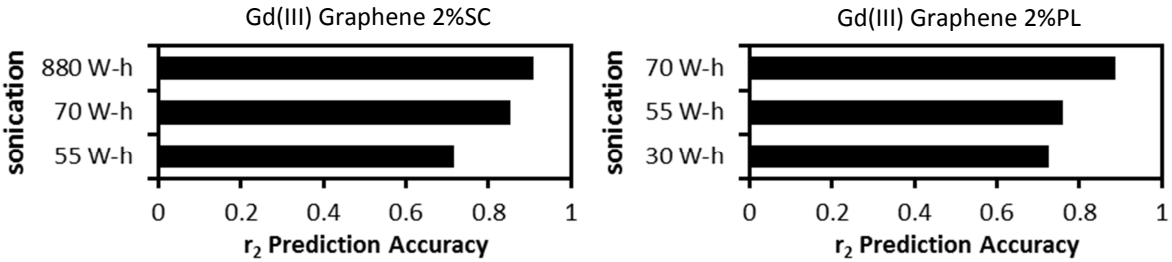

Figure S9. NMRD analysis of Gd(III) Graphene as a function of sonication. The analysis assumed that only local motions and electronic relaxation changed with sonication. q, τ_R, and τ_M were assumed to be constant. Several trends in the data suggest additional relaxivity-modulating parameters or mechanisms in pristine graphene that are unaccounted for in current theory. Specifically, 1) the decreasing T_{1e} (100 kHz) trend with sonication suggests that graphene damage may modulate electronic relaxation, 2) the opposite trends in S^2 between the 2%SC and the 2%PL samples seem implausible physically, and 3) the theory predicts r_2 with decreasing accuracy for the less sonicated, and presumably more pristine, gadographenes. The samples analyzed were Gd(III) Graphene 2%SC Preparation 2, 3, and 4A, and Gd(III) Graphene 2%PL Preparation 1, 2A, and 3. Gd(III) Graphene 2%SC Preparation 1 was excluded because 2, 3, and 4A all experienced significant aging whereas 1 did not. Gd(III) Graphene 2%PL Preparation 4A was excluded due to poor NMRD data quality as a result of low Gd(III) loading (Table S1).

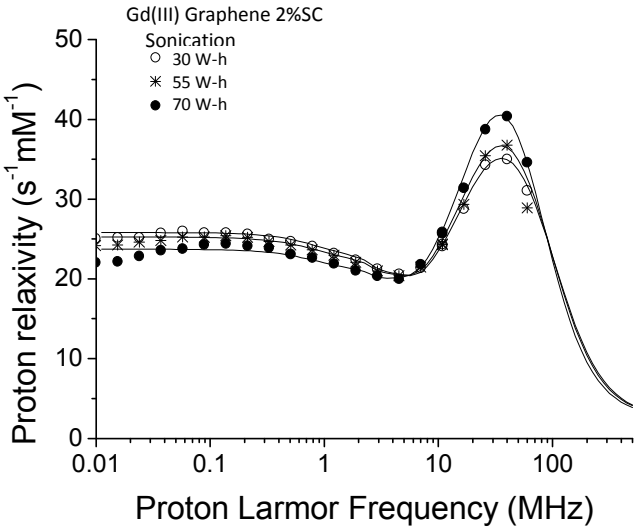

	Gd(III) Graphene 2%SC		
Sonication	55 W-h	70 W-h	880 W-h
τ_M	1.6	1.7	2.0
$T_{1e}^{100\ kHz}$(ps)	257	257	257
Δ_t (cm^{-1})	0.0195	0.0195	0.0195
τ_v (ps)	24	24	24
D_{ZFS} (cm^{-1})	0.05	0.05	0.05
Θ (^{o})	40	43	50
τ_{fast} (ps) (fixed)	12	12	12
Predicted r_2 ($mM^{-1}s^{-1}$)	43	45	50
Measured r_2 ($mM^{-1}s^{-1}$)	60	54	56

Fixed values: q=5, r =3.1 Å, d=3.8 Å, D=3.3 × 10^{-5} cm^2/s, $\tau_R \geq 1000$ ns, S^2=0.16

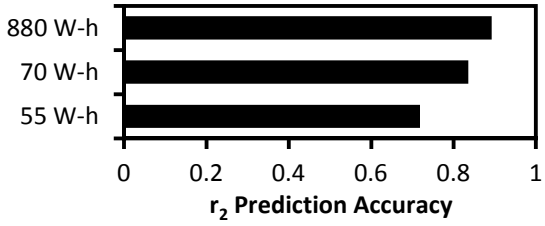

Figure S10. Alternative NMRD analysis of Gd(III) Graphene 2%SC as a function of sonication. The analysis assumed that only water exchange and electronic relaxation changed with sonication. The non-uniqueness of NMRD best-fits is demonstrated. The qualitative trend in r_2 prediction accuracy is consistent with the results in Figure S9.

4. Supplementary Notes

4.1 Supplementary discussion on the r_2 of gadographenes

The theoretical r_2 (60 MHz) of all gadographenes were calculated by SBM theory using the relaxometric parameters obtained from the analyses of their NMRD profiles. When graphene or reduced GO was used as the carbon scaffold, the r_2 of gadographenes were underestimated by 9% - 32%. This result held for both $GdCl_3$ and Gd(III)-complexes. Agreement between theory and experiment grew as sonication, and presumably the damage, applied to the materials increased. When GO, the oxidized form of graphene without itinerant electrons, was used as the carbon scaffold, the r_2 of gadographenes were predicted accurately by SBM theory (with Gd(III)-DTPA-GO being the single exception). These results show that the theoretical analyses performed fail to account for a portion of the r_2 in the samples with pristine graphene. Here, potential explanations that supplement the discussions in the main text are considered.

The r_2 calculated using theory includes contributions from dipole-dipole, scalar, and outer-sphere interactions, and chemical shift of the bound water protons. Typically, both the scalar interaction and the chemical shift are negligible because the metal-proton hyperfine coupling constant ($A/\hbar$) is small (eqs [S23], [S26], and [S27]). Similarly, in the usual case of unhindered water diffusion, outer-sphere effects are much smaller than inner-sphere effects. If $A/\hbar$ is greater or if water diffusion is slower in the samples with graphene than expected, then these contributions may be significant. For example, graphene tends to form stacks of a few layers in solution whereas GO tends to solvate as mono- and bi-layers; therefore, it is possible that water molecules diffusing between graphene sheets in a stack contribute outer-sphere or chemical shift r_2 effects that are not considered in the present analysis. However, it should be noted that these effects, excluding chemical shift difference (eqs [S17] and [S18]), do not elevate r_2 exclusively; they affect r_1, and in turn, the NMRD profiles, too.

Surfactants, carbon nanomaterials, and impurities are other potential contributors to the enhancement of relaxation rates. SC and PL were both shown to have a negligible effect on T_1 and T_2 (Table S6). The carbon nanomaterials and their associated impurities, most notably iron, were found to decrease T_1 and T_2, but to a much lesser extent than Gd(III). These contributions have been corrected for in all of the reported relaxivities. Therefore, it is unlikely for the relaxation effects of surfactants, carbon nanomaterials, or impurities to explain the larger-than-expected r_2 of gadographenes.

Another consideration is the non-uniqueness of the NMRD best-fits and the codependence among the different fitting parameters. Although the trend in r_2 prediction accuracy in the two scenarios we analyzed were consistent with each other (Figures S9 and S10), other best-fits remain possible.

Finally, due to the complexity of the gadographene system, it is important to consider non-measurement-related sources of error that can potentially add uncertainty to the interpretation of the results. First, as a nanomaterial, it is difficult to obtain an unequivocal structural characterization of gadographene. Based on the measured dissociation constants (10^{-8} – 10^{-10} M), it is likely that only a negligible amount of free Gd(III) is present as the Gd(III) concentrations of the samples are on the order of 10^{-5} M. However, no information is known about the Gd(III) coordination environment or the Gd(III) distribution (e.g. edge vs. plane) on the carbon nanomaterials. In addition, all analyses were done based on properties that emerge from ensemble averages without considering the population nature of nanomaterials. Secondly, as alluded to previously, the gadographene samples are a complex mixture of carbon nanomaterials, Gd(III) ions, impurities, and in the case of Gd(III) Graphene, surfactants. When correcting for contributions to relaxation time, we had normalized the corrections to either [C] or [Fe] of the individual samples (Table S1). Rigorously, relaxivity corrections should be done by individually subtracting the contributions from carbon, iron, surfactants, and other impurities. Unfortunately, this

method was not applicable because the isolated contribution from each of the different components is not known. With a few exceptions, all of the reported relaxivities were corrected based on iron because it is the second most important contributor to proton relaxation after Gd(III). For Gd(III) GO, corrections were done based on carbon because the measured iron concentrations in these samples were either below or only slightly above the ICP detection limit. For the NMRD profiles and the associated analyses in r_2 prediction accuracy, corrections were done using carbon because the NMRD profiles were not as flat as one would expect in the low field regions (< 1MHz) when corrections were done using iron. Ultimately, the qualitative trends in r_2 and its prediction accuracy by theory remained similar regardless of the correction method used.

Supplementary References

(1) Hernandez, Y.; Nicolosi, V.; Lotya, M.; Blighe, F. M.; Sun, Z. Y.; De, S.; McGovern, I. T.; Holland, B.; Byrne, M.; Gun'ko, Y. K.; Boland, J. J.; Niraj, P.; Duesberg, G.; Krishnamurthy, S.; Goodhue, R.; Hutchison, J.; Scardaci, V.; Ferrari, A. C.; Coleman, J. N. *Nat Nanotechnol* **2008**, *3*, 563.

(2) Sitharaman, B.; Kissell, K. R.; Hartman, K. B.; Tran, L. A.; Baikalov, A.; Rusakova, I.; Sun, Y.; Khant, H. A.; Ludtke, S. J.; Chiu, W.; Laus, S.; Toth, E.; Helm, L.; Merbach, A. E.; Wilson, L. J. *Chem Commun* **2005**, 3915.

(3) Kovtyukhova, N. I.; Ollivier, P. J.; Martin, B. R.; Mallouk, T. E.; Chizhik, S. A.; Buzaneva, E. V.; Gorchinskiy, A. D. *Chem Mater* **1999**, *11*, 771.

(4) Duch, M. C.; Budinger, G. R. S.; Liang, Y. T.; Soberanes, S.; Urich, D.; Chiarella, S. E.; Campochiaro, L. A.; Gonzalez, A.; Chandel, N. S.; Hersam, M. C.; Mutlu, G. M. *Nano Lett* **2011**, *11*, 5201.

(5) Liu, Z.; Robinson, J. T.; Sun, X. M.; Dai, H. J. *J Am Chem Soc* **2008**, *130*, 10876.

(6) Fernandez-Merino, M. J.; Guardia, L.; Paredes, J. I.; Villar-Rodil, S.; Solis-Fernandez, P.; Martinez-Alonso, A.; Tascon, J. M. D. *J Phys Chem C* **2010**, *114*, 6426.

(7) Rourke, J. P.; Pandey, P. A.; Moore, J. J.; Bates, M.; Kinloch, I. A.; Young, R. J.; Wilson, N. R. *Angew Chem Int Edit* **2011**, *50*, 3173.

(8) Essien, H.; Lai, J. Y.; Hwang, K. J. *J Med Chem* **1988**, *31*, 898.

(9) Chadwick, J.; Jones, M.; Mercer, A. E.; Stocks, P. A.; Ward, S. A.; Park, B. K.; O'Neill, P. M. *Bioorgan Med Chem* **2010**, *18*, 2586.

(10) Manus, L. M.; Mastarone, D. J.; Waters, E. A.; Zhang, X. Q.; Schultz-Sikma, E. A.; MacRenaris, K. W.; Ho, D.; Meade, T. J. *Nano Lett* **2010**, *10*, 484.

(11) Wang, B.; Luo, B.; Liang, M.; Wang, A.; Wang, J.; Fang, Y.; Chang, Y.; Zhi, L. *Nanoscale* **2011**, *3*, 5059.

(12) Wang, S.; Chia, P. J.; Chua, L. L.; Zhao, L. H.; Png, R. Q.; Sivaramakrishnan, S.; Zhou, M.; Goh, R. G. S.; Friend, R. H.; Wee, A. T. S.; Ho, P. K. H. *Advanced Materials* **2008**, *20*, 3440.

(13) Bourlinos, A. B.; Gournis, D.; Petridis, D.; Szabo, T.; Szeri, A.; Dekany, I. *Langmuir* **2003**, *19*, 6050.

(14) Compton, O. C.; Dikin, D. A.; Putz, K. W.; Brinson, L. C.; Nguyen, S. T. *Adv Mater* **2010**, *22*, 892.

(15) Lauffer, R. B. *Chem Rev* **1987**, *87*, 901.

(16) Wang, Z. X. *Febs Lett* **1995**, *360*, 111.

(17) Caravan, P.; Ellison, J. J.; McMurry, T. J.; Lauffer, R. B. *Chem Rev* **1999**, *99*, 2293.

(18) Bianchi, A.; Calabi, L.; Corana, F.; Fontana, S.; Losi, P.; Maiocchi, A.; Paleari, L.; Valtancoli, B. *Coordin Chem Rev* **2000**, *204*, 309.

(19) Harris, D. C. In *Quantitative Chemical Analysis*; 8th ed.; W. H. Freeman and Co: New York, 2010, p 242.

(20) Djanashvili, K.; Peters, J. A. *Contrast Media Mol I* **2007**, *2*, 67.

(21) de la Torre, J. G.; Huertas, M. L.; Carrasco, B. *J Magn Reson* **2000**, *147*, 138.

(22) Solomon, I. *Phys Rev* **1955**, *99*, 559.

(23) Bloembergen, N. *J Chem Phys* **1957**, *27*, 572.

(24) Bloembergen, N.; Morgan, L. O. *J Chem Phys* **1961**, *34*, 842.

(25) Kowalewski, J.; Kruk, D.; Parigi, G. *Adv Inorg Chem* **2005**, *57*, 41.

(26) Bertini, I.; Galas, O.; Luchinat, C.; Parigi, G. *J Magn Reson Ser A* **1995**, *113*, 151.

(27) Bertini, I.; Kowalewski, J.; Luchinat, C.; Nilsson, T.; Parigi, G. *J Chem Phys* **1999**, *111*, 5795.

(28) Bertini, I.; Luchinat, C.; Parigi, G. *Adv Inorg Chem* **2005**, *57*, 105.

(29) Caravan, P.; Parigi, G.; Chasse, J. M.; Cloutier, N. J.; Ellison, J. J.; Lauffer, R. B.; Luchinat, C.; McDermid, S. A.; Spiller, M.; McMurry, T. J. *Inorg Chem* **2007**, *46*, 6632.

(30) Li, W. H.; Parigi, G.; Fragai, M.; Luchinat, C.; Meade, T. J. *Inorg Chem* **2002**, *41*, 4018.

(31) Major, J. L.; Parigi, G.; Luchinat, C.; Meade, T. J. *P Natl Acad Sci USA* **2007**, *104*, 13881.

(32) Mastarone, D. J.; Harrison, V. S. R.; Eckermann, A. L.; Parigi, G.; Luchinat, C.; Meade, T. J. *J Am Chem Soc* **2011**, *133*, 5329.

(33) Jones, J. E.; Amoroso, A. J.; Dorin, I. M.; Parigi, G.; Ward, B. D.; Buurma, N. J.; Pope, S. J. A. *Chem Commun* **2011**, *47*, 3374.

(34) Anelli, P. L.; Bertini, I.; Fragai, M.; Lattuada, L.; Luchinat, C.; Parigi, G. *Eur J Inorg Chem* **2000**, 625.

(35) Kowalewski, J.; Luchinat, C.; Nilsson, T.; Parigi, G. *J Phys Chem A* **2002**, *106*, 7376.

(36) Lipari, G.; Szabo, A. *J Am Chem Soc* **1982**, *104*, 4546.

(37) Hwang, L. P.; Freed, J. H. *J Chem Phys* **1975**, *63*, 4017.
(38) Freed, J. H. *J Chem Phys* **1978**, *68*, 4034.
(39) Caravan, P.; Greenfield, M. T.; Bulte, J. W. M. *Magnet Reson Med* **2001**, *46*, 917.
(40) Ashcroft, N. W.; D., M. N. In *Solid State Physics*; Brooks Cole: Belmont, CA, 1976, p 675.